New Frontiers For Interaction-Induced States

IPSITA MANDAL

THE HENRYK NIEWODNICZAŃSKI
INSTITUTE OF NUCLEAR PHYSICS
POLISH ACADEMY OF SCIENCES

NORDITA
The Nordic Institute for
Theoretical Physics

Research Portfolio

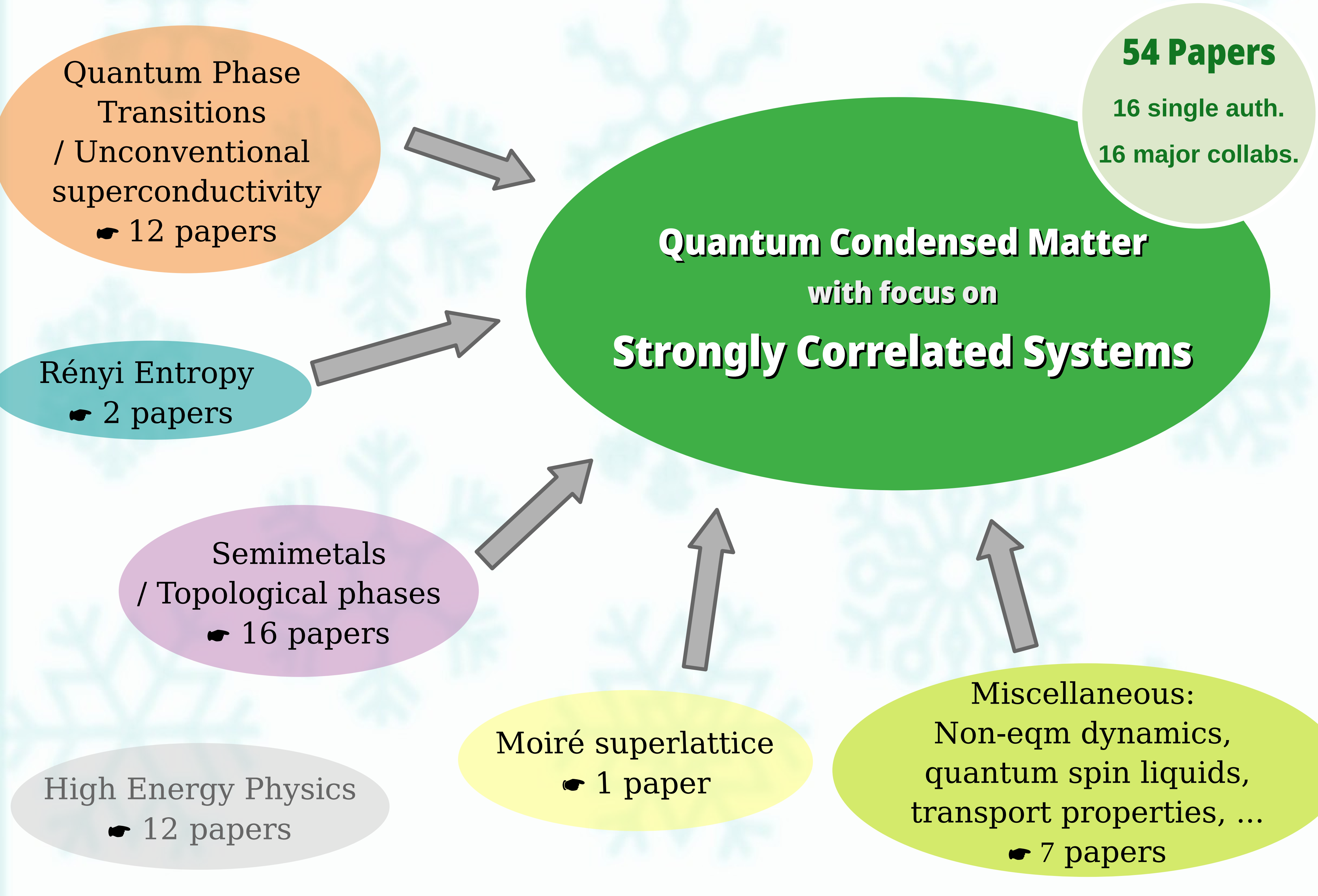

Focal Points

Strange Metals
or
Non-Fermi liquids

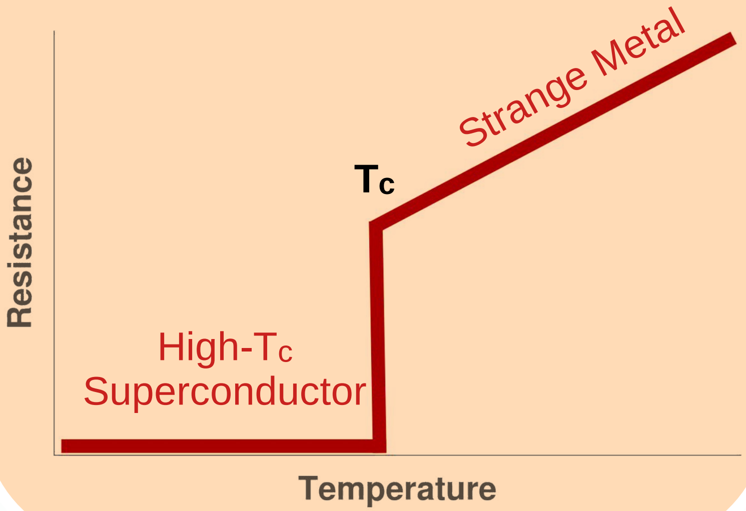

2d multi-layers
☛ Moiré superlattices

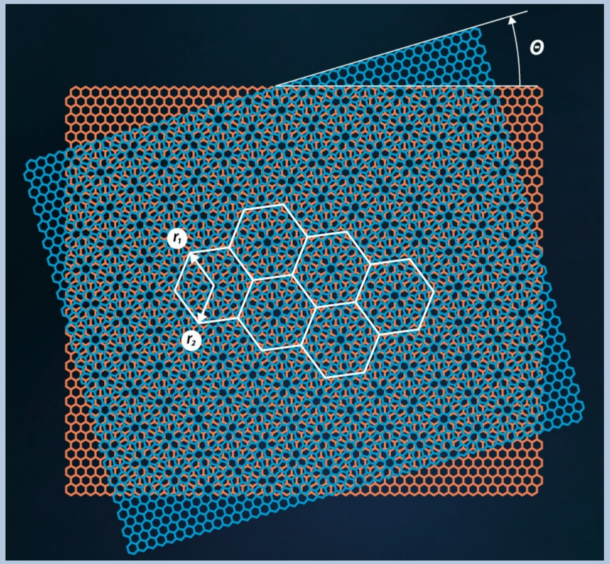

MIPT

Strange Metals from Quantum Critical Points

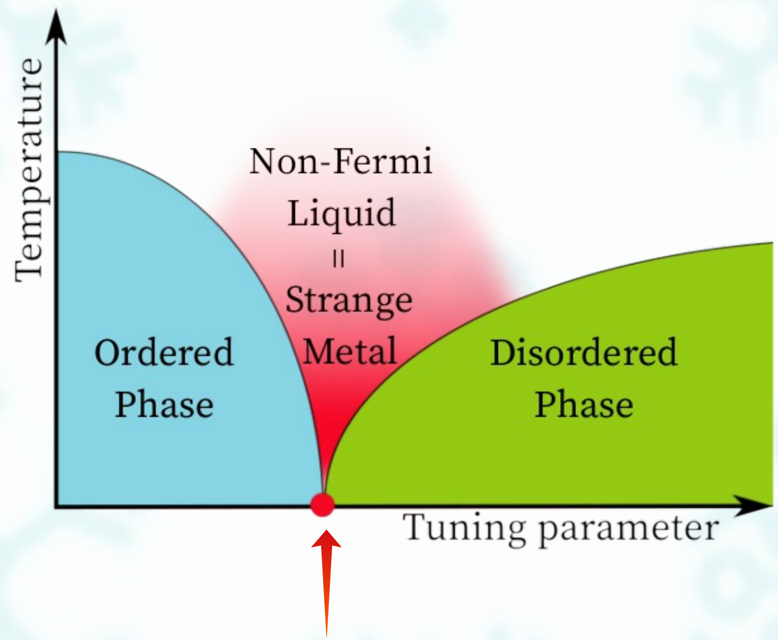

Quantum Critical Point

Theory of Normal Metals

Landau

Fermi Liquid (FL) ☛ Properties of finite density interacting fermions don't depend on specific microscopic details

- **Ground state** ☛ characterized by a sharp Fermi surface (FS) in momentum space
- **Quasiparticles** ☛ low energy excitations near FS

FS ☛ jump in fermion occupation number n(k) at T=0

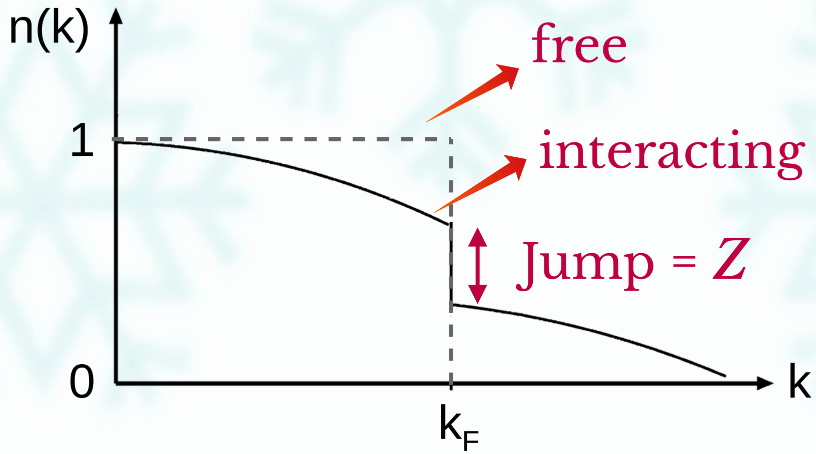

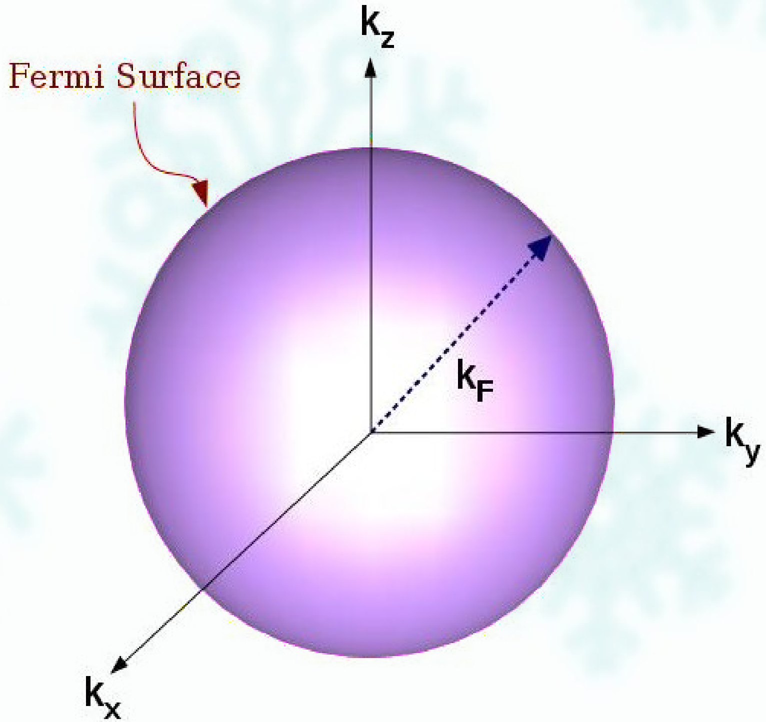

Quasiparticles: Emergent Entities in FL

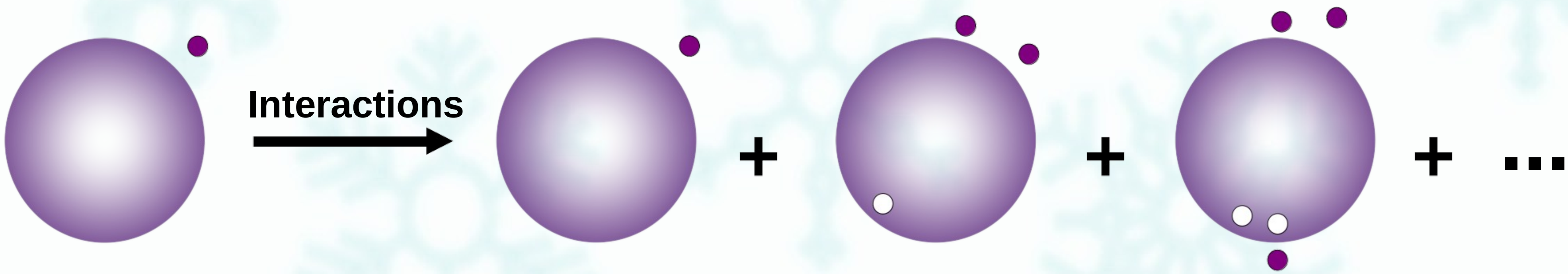

Coherent part of
single-particle Green's function

$$G_R(\omega, \mathbf{k}) = \frac{Z}{\omega - v_F\, k_\perp - k_\parallel^2 + i\,\Gamma}$$

$$\omega = E - E_F\,, \quad k_\perp = k - k_F$$

Quasiparticles

☛ collective low energy quantum oscillations

- ✓ Quasiparticle lifetime diverges close to FS ☛ Decay rate $\Gamma \sim \omega^2$
- ✓ Overlap between elementary excitations of free and interacting systems ☛ quasiparticle weight $0 < Z \leq 1$

Manifestation of FL

- Ground state adiabatically connected to the non-interacting problem
- Quasiparticles $\xleftrightarrow{\text{one-to-one}}$ free system excitations
- Temperature (T) dependence of thermodynamic & transport properties similar to free fermions

> - **Resistivity $\rho \propto T^2$**
> - **Specific heat $\propto T$**
> - **Im (self energy Σ) $\propto \omega^2$**

A complicated problem reduced to a simpler one

Breakdown of FL Theory

Long-lived quasiparticles

☛ FL

Massive

Boson

Electrons + Bosons

↓

Low energy QFT

Massless

Boson

No quasiparticle

☛ non-Fermi liquid (**NFL**)

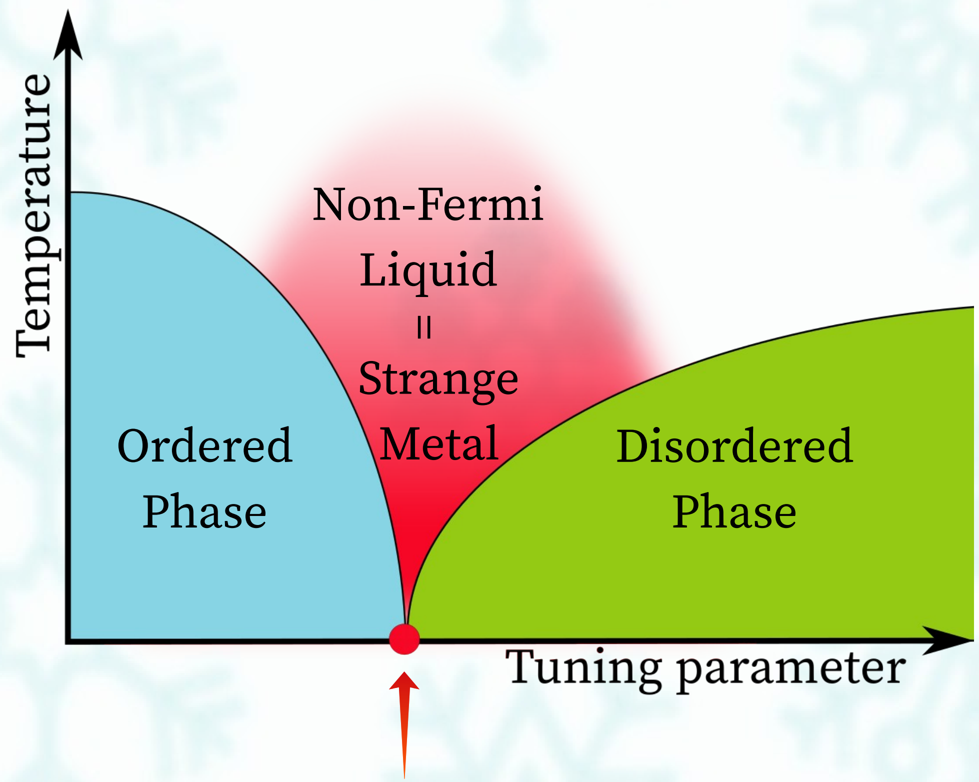

Bosonic order parameter massless at Quantum Critical Point (**QCP**)

mediates

strong interactions

e.g. Antiferro order,
nematic order,
charge density order,
gauge fields ...

Quantum Critical Metal

Recipe for NFL as fermion-boson coupling becomes strong in 2d, even if bare coupling is weak ☛ $Z \to 0$ ☛ quasiparticles destroyed

FL **FS away from QCP**

NFL **FS at QCP**

Critical fluctuations at QCP coupled to itinerant electrons (FS)

Attempt to describe NFL as

FS + Gapless Order Parameter fluctuations

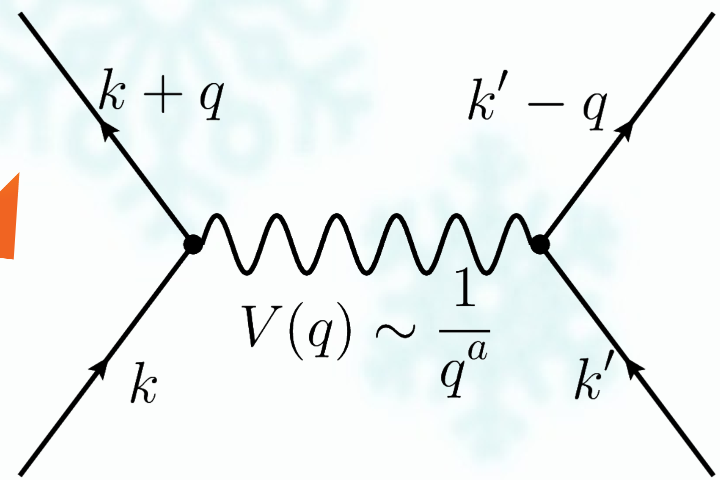

Where do NFLs Appear?

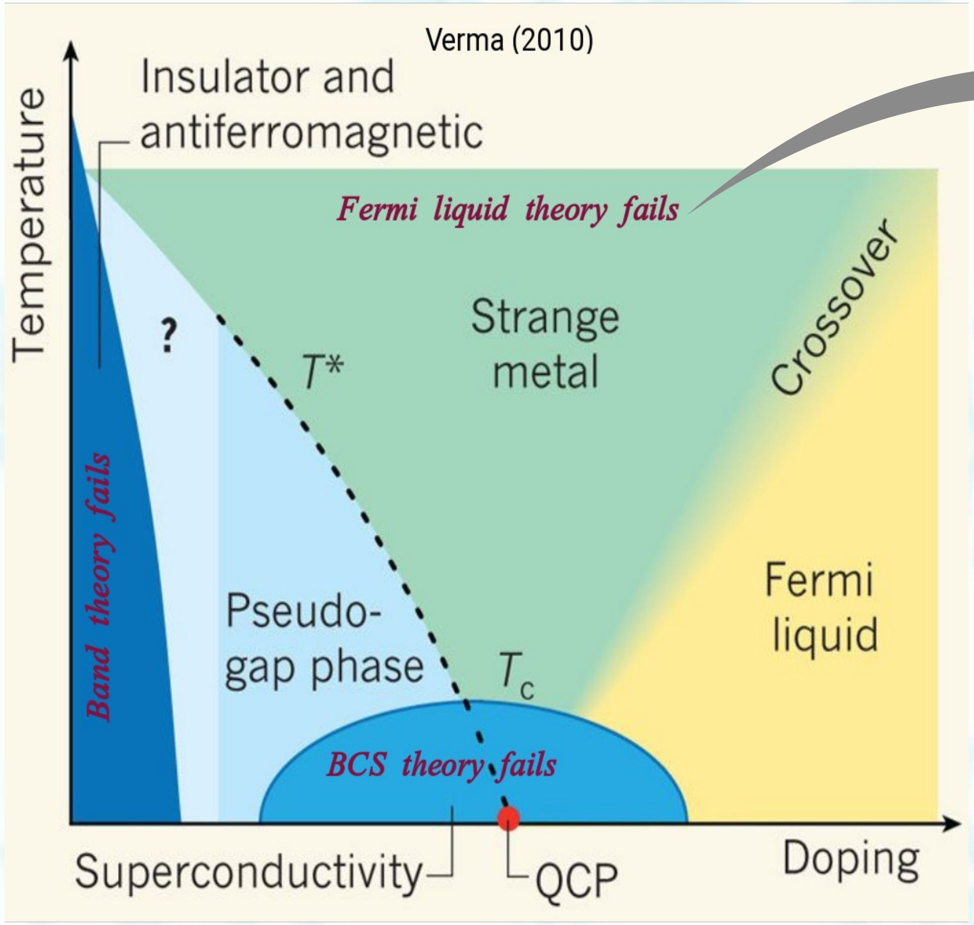

Phase diagram of high-T_c cuprates

Non-Fermi Liquid (NFL) metals

- $\rho \propto T$
- $\mathrm{Im}\,\Sigma \propto \omega$ in ARPES
- No Landau quasiparticles

NFLs: How to Explain Theoretically?

We developed a novel analytical framework

QFT

Dimensional Regularization + Renormalization Group

[**IM** & S-S Lee, *PRB (2015)*]

Our controlled approximation allowed to compute critical exponents, optical conductivity, …

NFLs: Dimensional Regularization

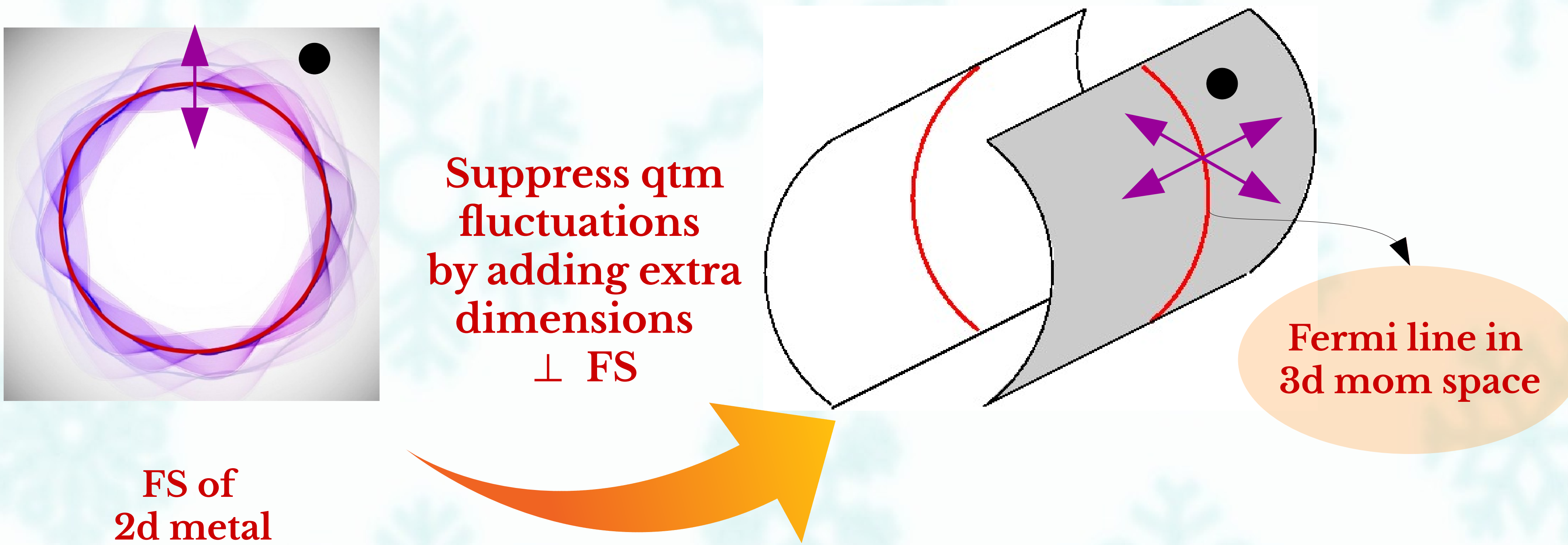

- Find upper critical dimension $\mathbf{d_c}$ such that $\mathbf{d} > \mathbf{d_c}$ described by mean-field theory (FL) ☛ well-known tool from Statistical Mechanics / QFT
- $\mathbf{d_{phys}} \leq \mathbf{d_c}$ ☛ mean-field theory inapplicable
  ☛ carry out perturbation in $\epsilon = d_c - d_{phys}$

Applications: Ising-Nematic QCP

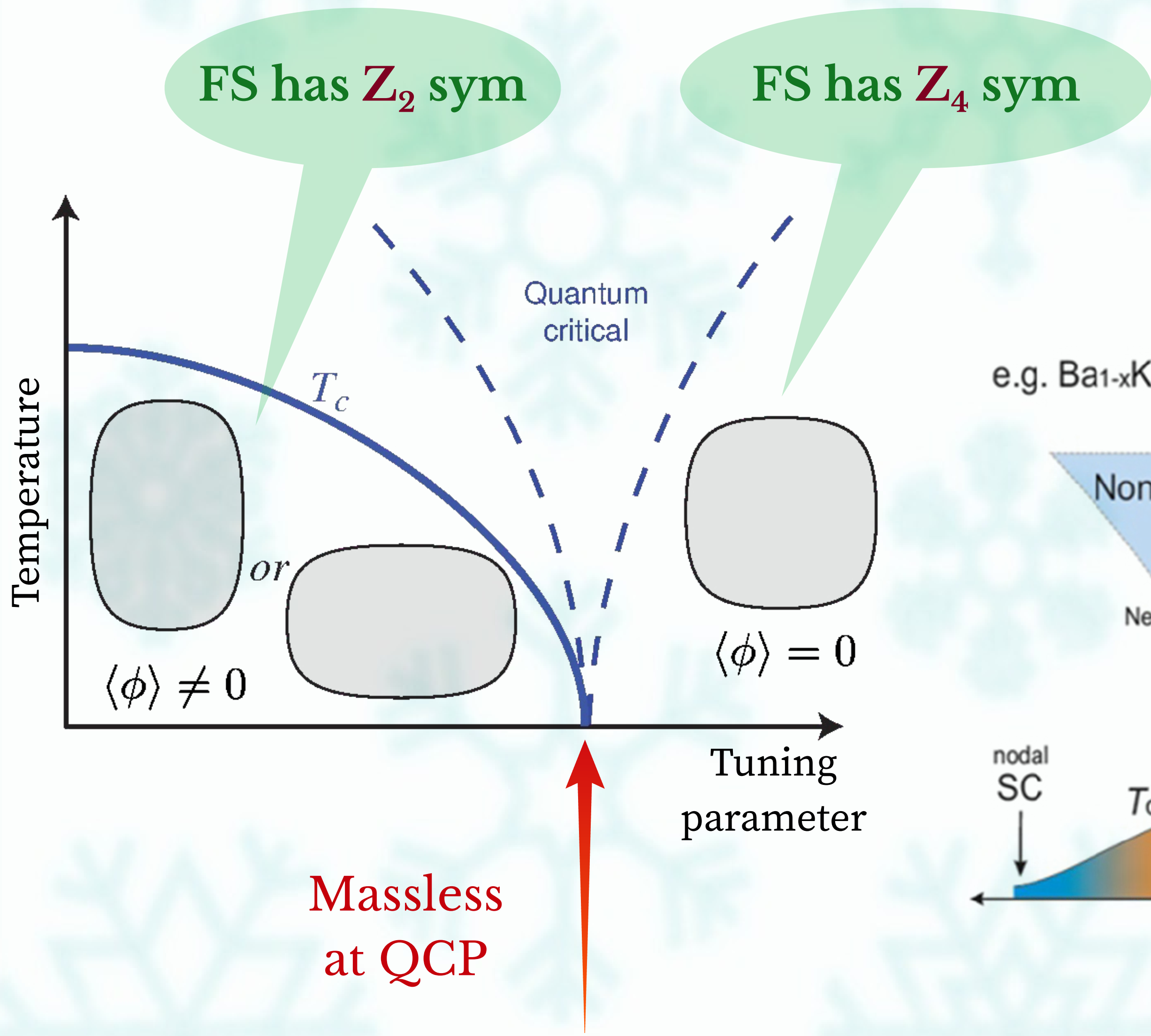

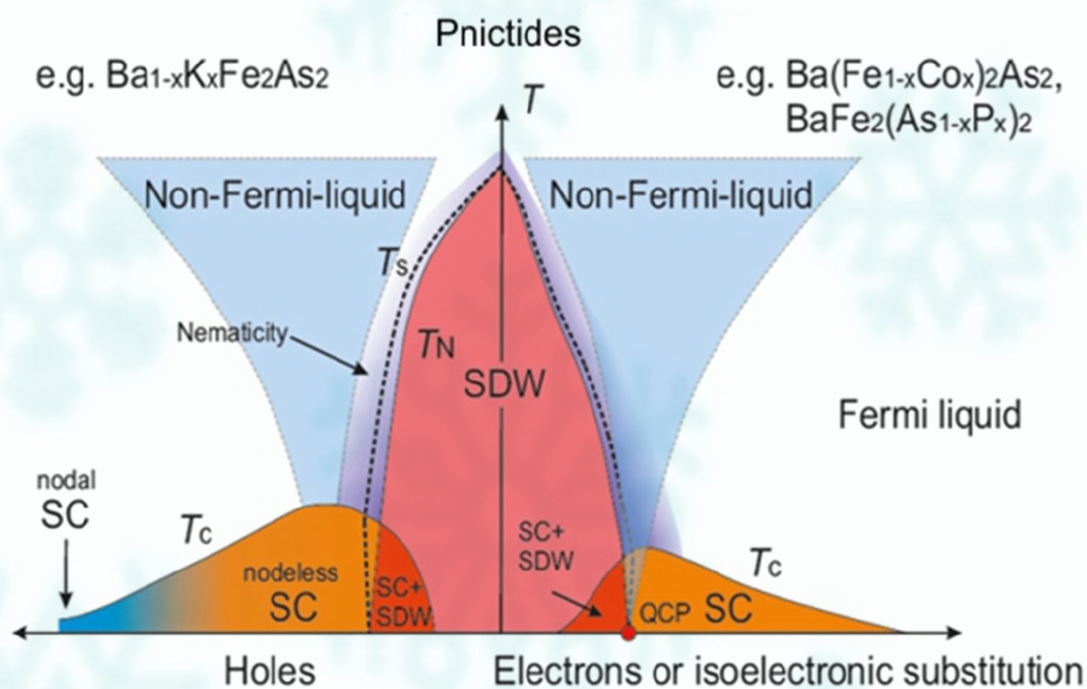

Order Parameter ϕ ☛ Real Scalar Boson

[**$YBa_2Cu_3O_y$** (Cuprate), **$Sr_3Ru_2O_7$** (Ruthenate), **Pnictides**]

Results: 2d Ising-Nematic QCP

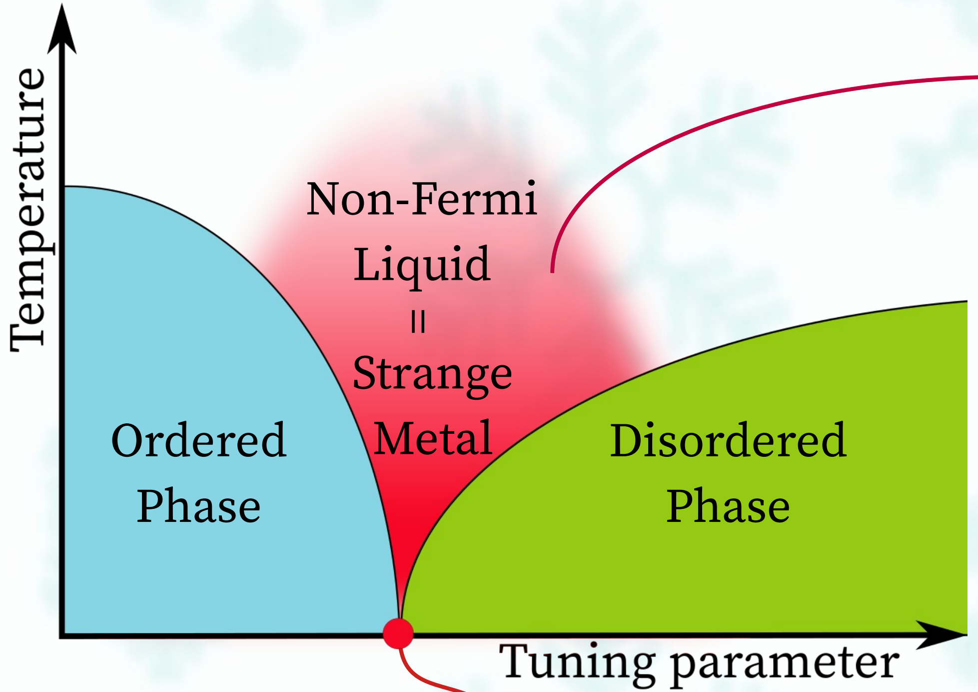

1d FS fluctuations
effectively local

Optical conductivity

$\sigma(\omega) \sim \omega^{-2/3}$

☛ close to $\omega^{-0.65}$ found in expts.
on optimally doped cuprates

[A. Eberlein, **IM**, & S. Sachdev, *PRB (2016)*]

Massless Boson at

Quantum Critical Point

Results: 2d Ising-Nematic QCP

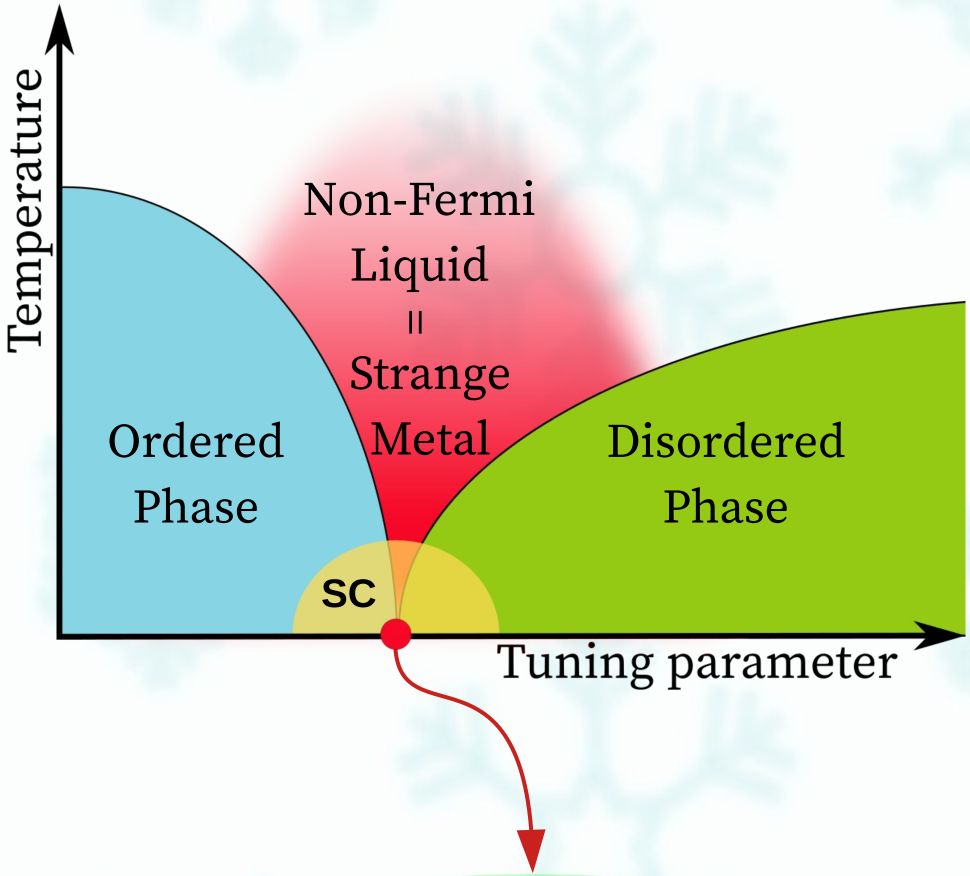

Quantum Critical Point masked by superconducting (SC) dome

Competition between non-Fermi liquid phase & pairing instability at T=0

☛ **Superconductivity (SC) wins**

[**IM**, *PRB (2016)*]

Results: 3d Ising-Nematic QCP

2d FS fluctuations
non-local
☛ entangled all over the FS

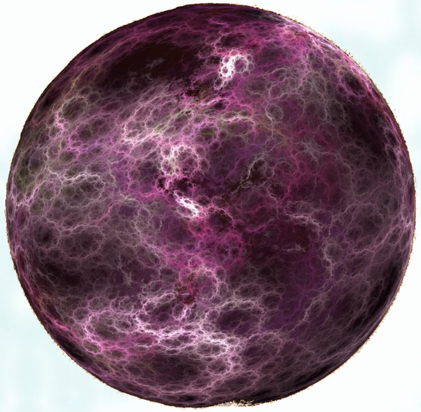

- Fluctuations less violent than 1d FS
- Ultraviolet / Infrared mixing
- ≥ 2-loop corrections vanish

[**IM** & S-S Lee, *PRB (2015)*]

[**IM**, *EPJB (2016)*]

Technical Details
for
Ising-Nematic QCP

m-dim FS + Scalar Boson

Low energy limit ☛ Fermions scatter tangentially

Time-Reversal Invariance assumed

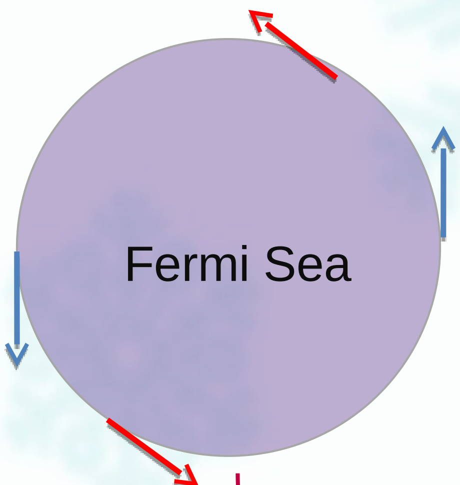

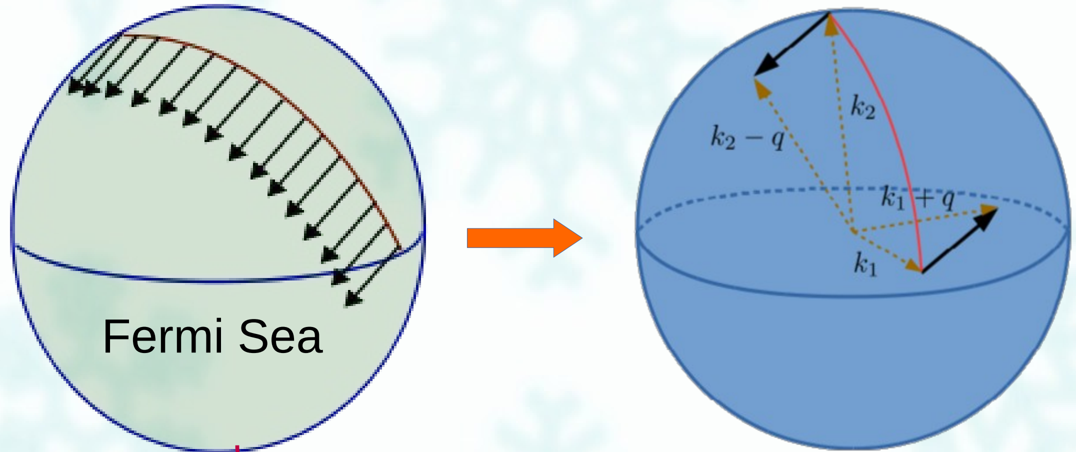

Circular FS (m=1)

☛ fermions in different patches

decoupled except

antipodal points

Not true for

m-dim FS

with m > 1

Size of FS (k_F) enters as a dimensionful parameter

Significance of m

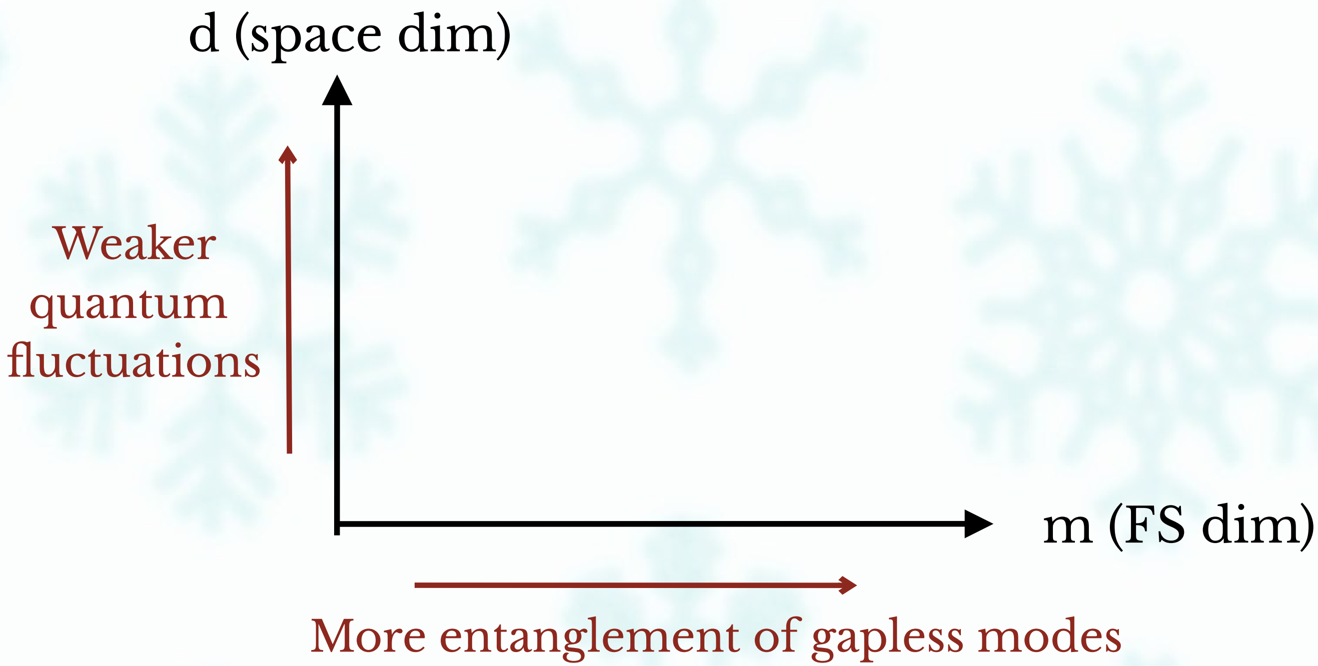

- m = 1 ☛ observables local in mom space (e.g. Green's fns) can be extracted from local patches ☛ emergent locality

  [D. Dalidovich & S-S. Lee, *Phys. Rev. B 88, 245106 (2013)*]

- m > 1 ☛ UV/IR mixing ☛ low-energy physics affected by gapless modes on entire FS ☛ size of FS (k_F) modifies naive scaling coming from patch description ☛ k_F becomes a 'naked scale'

  [**IM** & S-S Lee, *Phys. Rev. B 92, 035141 (2015)*]

Coordinate Set-up

Patch of m-dim FS of arbitrary shape

$d = d_{phys} = m + 1$

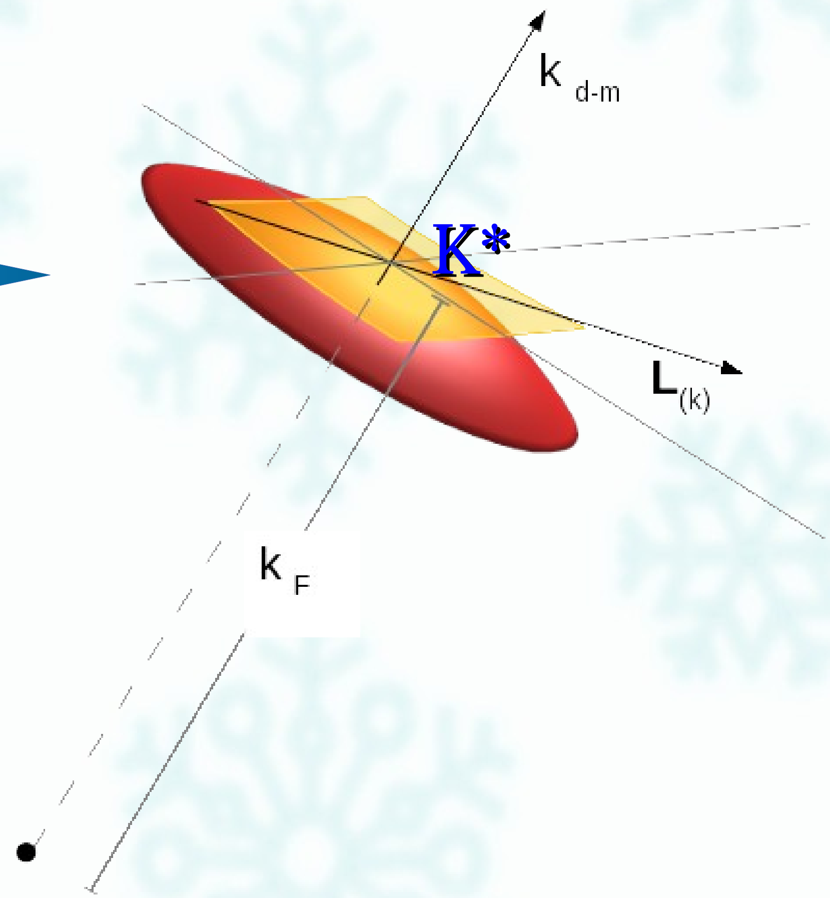

- At a chosen point K* on FS : $k_{d\text{-}m} \perp$ local S^m ☛ its magnitude measures deviation from k_F
- $L_{(k)} = (k_{d\text{-}m+1} , k_{d\text{-}m+2} ,..., k_d)$ ☛ tangential along the local S^m

Fermions on Antipodal Points

Time-Reversal Invariance assumed

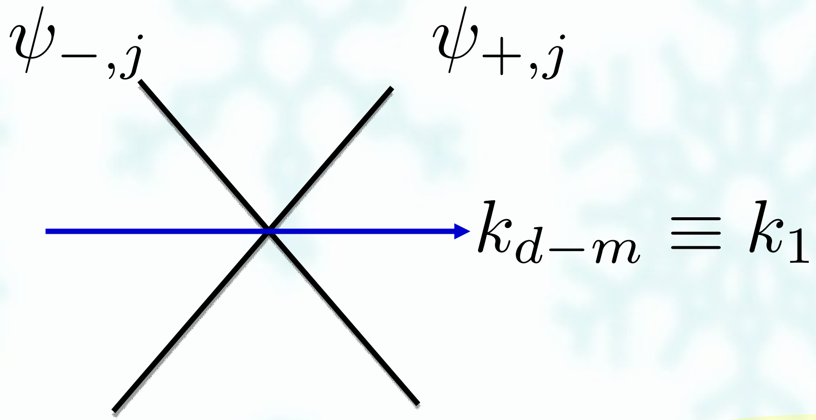

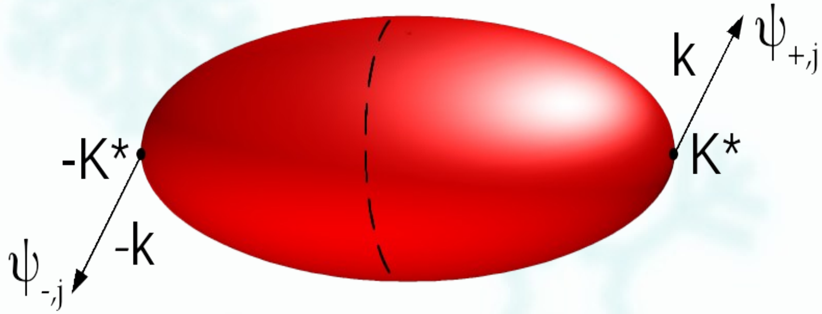

$$\psi_{+,j}\,(\psi_{-,j})$$

right (left) moving fermion
with flavour j=1,2,...,N

Effective Action

2 halves of m-dim FS
+ massless boson
in **d** space
& one time dim

d = d_{phys} = m + 1

$$S = \sum_{s=\pm,j} \int \frac{d^{m+2}k}{(2\pi)^{m+2}} \, \psi^\dagger_{s,j}(k) \Big[\mathrm{i}\, k_0 + s\, k_{d-m} + \mathbf{L}^2_{(k)} \cancel{+ \mathcal{O}\big(|\mathbf{L}_{(k)}|^3\big)} \Big] \psi_{s,j}(k)$$

$$+ \frac{1}{2} \int \frac{d^{m+2}k}{(2\pi)^{m+2}} \left[k_0^2 + k_1^2 + \mathbf{L}^2_{(k)} \right] \phi(-k)\, \phi(k)$$

$$+ \frac{e}{\sqrt{N}} \sum_{s=\pm,j} \int \frac{d^{m+2}k\, d^{m+2}q}{(2\pi)^{2m+4}} \, \phi(q)\, \psi^\dagger_{s,j}(k+q)\, \psi_{s,j}(k)$$

Action in terms of Dirac Fermions

$$\Psi_j(k) = \begin{pmatrix} \psi_{+,j}(k) \\ \psi^\dagger_{-,j}(-k) \end{pmatrix}$$

Interpret $|\mathbf{L}_{(k)}|$ as a continuous flavour

☛ each (m+2)-d spinor can be viewed as a (1+1)-d Dirac fermion

$$S = \sum_j \int \frac{d^{m+2}k}{(2\pi)^{m+2}} \, \bar{\Psi}_j(k) \, \mathrm{i} \left[\gamma_0 \, k_0 + \gamma_1 \left(k_{d-m} + \mathbf{L}^2_{(k)} \right) \right] \Psi_j(k)$$

$$+ \frac{1}{2} \int \frac{d^{m+2}k}{(2\pi)^{m+2}} \, \mathbf{L}^2_{(k)} \, \phi(-k) \, \phi(k)$$

$$+ \frac{\mathrm{i} \ e}{\sqrt{N}} \sum_j \int \frac{d^{m+2}k \, d^{m+2}q}{(2\pi)^{2m+4}} \, \phi(q) \, \bar{\Psi}_j(k+q) \, \gamma_{d-m} \Psi_j(k)$$

Embed FS in Higher Dimensions

Add extra spatial dimensions ⊥ $L_{(k)}$

☛ d > d_{phys}

$$k_0 \to \mathbf{K} \equiv (k_0, k_1, \ldots, k_{d-m-1})$$

$$\gamma_0 \to \Gamma \equiv (\gamma_0, \gamma_1, \ldots, \gamma_{d-m-1})$$

$$\gamma_1 \to \gamma_{d-m}$$

$$\delta_k \equiv k_{d-m} + \mathbf{L}^2_{(k)}$$

$$S = \sum_j \int \frac{d^{d+1}k}{(2\pi)^{d+1}} \bar{\Psi}_j(k)\, \mathrm{i} \left[\mathbf{\Gamma} \cdot \mathbf{K} + \gamma_{d-m}\, \delta_k \right] \Psi_j(k)$$

$$+ \frac{1}{2} \int \frac{d^{d+1}k}{(2\pi)^{d+1}} \mathbf{L}^2_{(k)}\, \phi(-k)\, \phi(k)$$

$$+ \frac{\mathrm{i}\, e}{\sqrt{N}} \sum_j \int \frac{d^{d+1}k\, d^{d+1}q}{(2\pi)^{2d+2}} \phi(q)\, \bar{\Psi}_j(k+q)\, \gamma_{d-m} \Psi_j(k)$$

Energy Scales

- Λ is implicit UV cut-off with K, k_{d-m} $<< \Lambda << k_F$

- k_F ☛ sets FS size
  Λ ☛ sets the largest momentum fermions can have $\perp$ FS

- Renormalization Group (RG) flows ☛ change Λ
  & require low-energy observables independent of Λ

- Fix **m** & tune **d** towards d_c at which fermion self-energy diverges logarithmically in Λ ☛ access NFL perturbatively in $\epsilon = d_c - (m+1)$

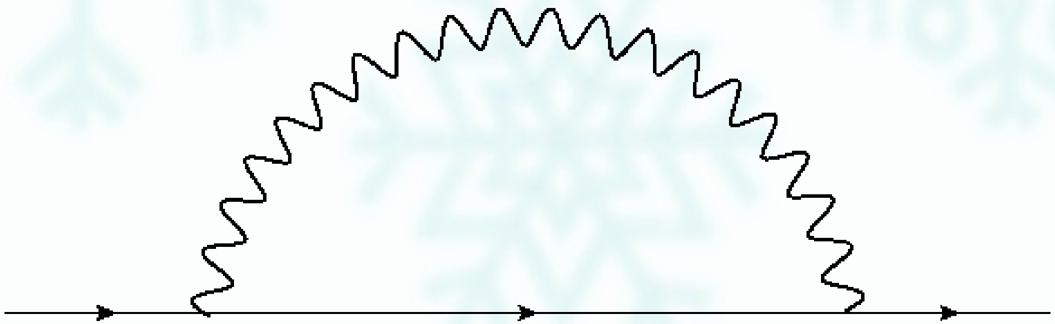

Critical Dimension

- Upper critical dim ☛ $$d_c = m + \frac{3}{m+1}$$

$d_c = 3$ for ($m = 2$, $d_{phys} = 3$)

$d_c = 5/2$ for ($m = 1$, $d_{phys} = 2$)

- Scaling dim of e = $1 - d/2 + m/4$

- e has positive scaling dimension at d_c for $1 < m < 2$
  ☛ cannot be the control parameter in perturbative loop expansions

- $$\mathrm{e}_{eff} = e^{\frac{2(m+1)}{3}} / \tilde{k}_F^{\frac{(m-1)(2-m)}{6}} \qquad \left(\tilde{k}_F = k_F/\Lambda\right)$$

has scaling dimension $[\, m + 3/(m+1) - d \,]\,(m+1)/3$ that vanishes at d_c

☛ effective coupling that is control parameter in loop expansions

One-Loop Results

Effective coupling

control parameter in loop expansions

$$e_{eff} = e^{\frac{2(m+1)}{3}} / \tilde{k}_F^{\frac{(m-1)(2-m)}{6}}$$

Fixed points of beta-function

$$\tilde{\beta} \equiv \frac{\partial e_{eff}}{\partial \ln \mu} = \frac{(m+1)(u_1\, e_{eff} - N\epsilon)\, e_{eff}}{3N - (m+1)u_1\, e_{eff}} = 0$$

Interacting Fixed Point

$$e^*_{eff} = \frac{N\epsilon}{u_1}$$

$$z^* = 1 + \frac{(m+1)\,\epsilon}{3}$$

$$\eta^*_\psi = \eta^*_\phi = -\frac{\epsilon}{2}$$

Dynamical critical exponent

Anomalous dimensions for fermions & boson

Two-Loop Boson Self-Energy

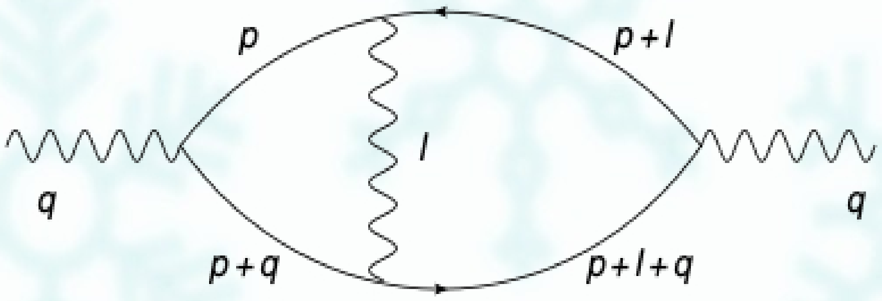

- For m > 1 ☛ k_F suppressed ☛ no correction

$$\Pi_2(q) \quad \sim \quad \frac{e^2\, k_F^{\frac{m-1}{2}}\, \pi^2}{6\, N\, |\vec{L}_{(q)}|^2\, \sin\left(\frac{m\,\pi}{3}\right)}\; \frac{e_{eff}^{\frac{m}{m+1}}}{k_F^{\frac{m-1}{2\,(m+1)}}}$$

- For m = 1 ☛ UV-finite correction

$$\Pi_2(q) \sim \left(\frac{e^2}{N\,|L_{(q)}|}\right) e_{eff}$$

Two-Loop Fermion Self-Energy

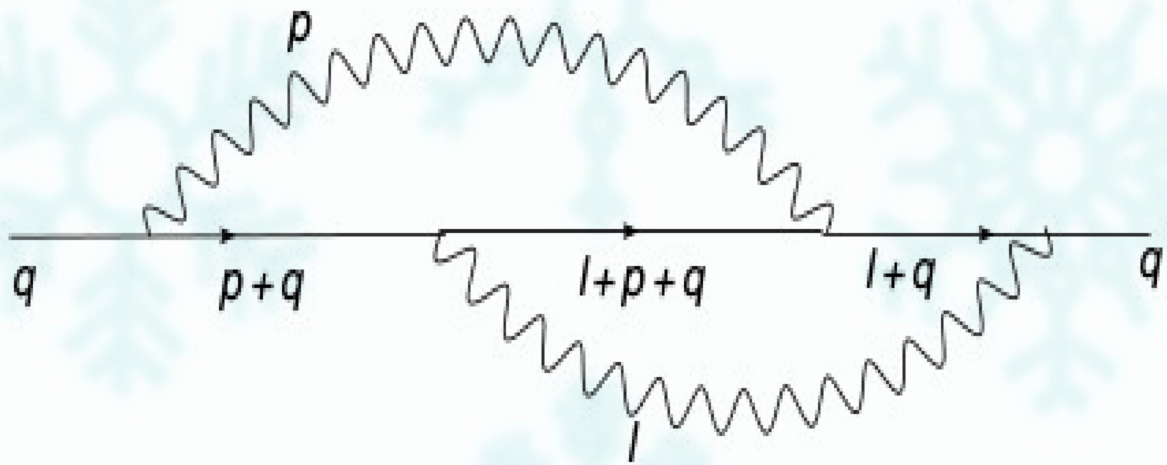

- For m > 1 ☛ $\Sigma_2(q) \quad \sim \quad k_F - suppressed$

  ☛ no correction

- For m = 1 ☛ UV-divergent

Pairing Instabilitites of Critical FS

FL unstable to arbitrary weak -ve interaction
in BCS channel leading to Cooper pairs
☛ How about a critical FS ?

[**IM**, *Phys. Rev. B 94, 115138 (2016)*]

Superconducting Instability

Add relevant 4-fermion terms
For simplicity, we consider s-wave case with 2 flavours

coupling constant

$$
\begin{aligned}
S^{\text{SC}} &= \frac{\mu^{d_v} V_S}{4} \sum_{j_1, j_2} \int \left(\prod_{s=1}^{4} dp_s \right) (2\pi)^{d+1}\, \delta^{(d+1)}(p_1 + p_2 - p_3 - p_4)\, (\delta_{j_1, j_2} - 1) \\
&\quad \times \left[\{ \bar{\Psi}_{j_1}(p_3) \Psi_{j_2}(p_1) \} \{ \bar{\Psi}_{j_2}(p_4) \Psi_{j_1}(p_2) \} - \{ \bar{\Psi}_{j_1}(p_3) \sigma_z \Psi_{j_2}(p_1) \} \{ \bar{\Psi}_{j_2}(p_4) \sigma_z \Psi_{j_2}(p_1) \} \right]
\end{aligned}
$$

Coupled Beta-Functions for V_s & e_{eff}

RG flows to $V_s \to -\infty$ for any initial V_s

☛ More susceptible to pairing than FL ($e_{eff} = 0$)

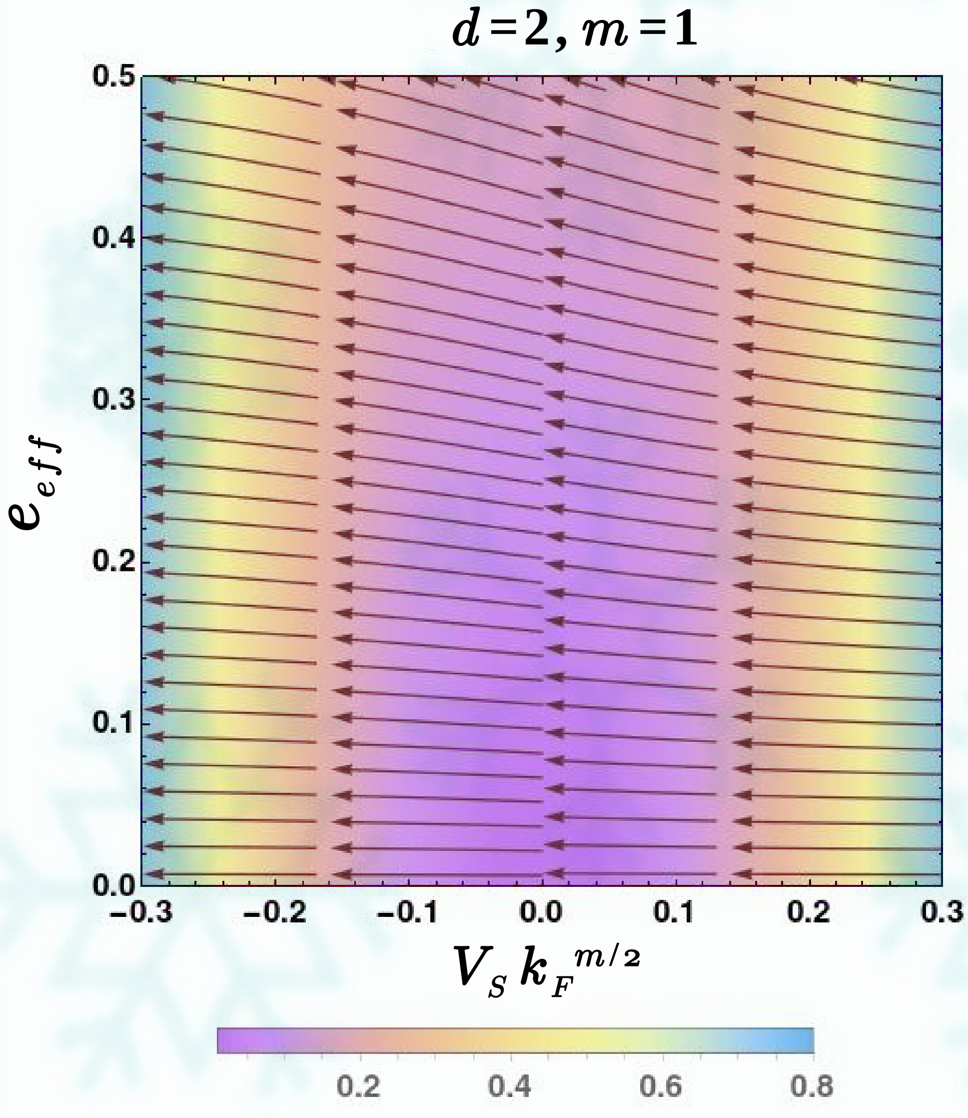

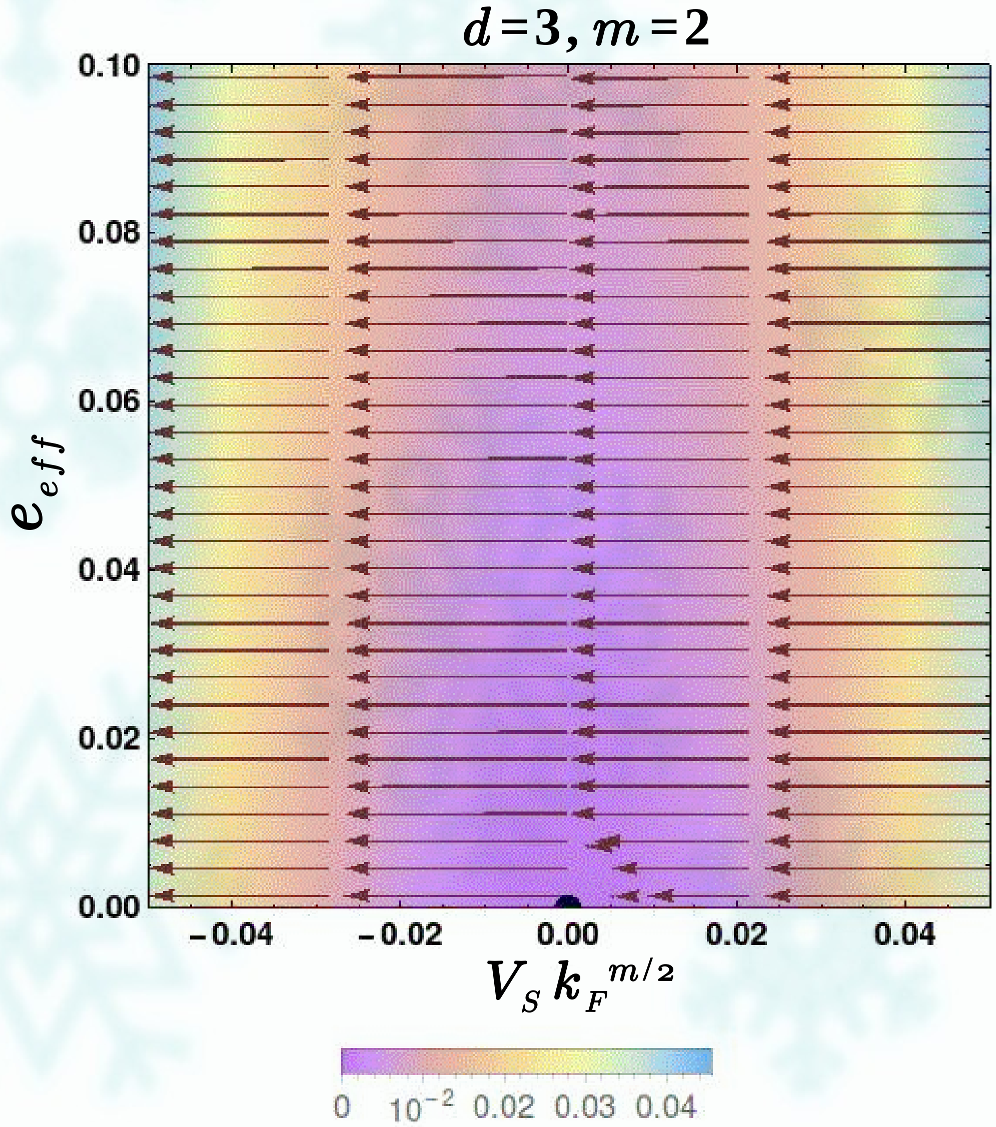

Fermi Surface
+
Transverse Gauge Field(s)

Fermi Surface + U(1) Gauge Field

$$S = \sum_j \int \frac{d^{d+1}k}{(2\pi)^{d+1}}\, \bar{\Psi}_j(k)\, \mathrm{i}\left[\boldsymbol{\Gamma}\cdot\mathbf{K} + \gamma_{d-m}\,\delta_k\right]\Psi_j(k)$$

$$+ \frac{1}{2}\int \frac{d^{d+1}k}{(2\pi)^{d+1}}\, \mathbf{L}^2_{(k)}\, \phi(-k)\,\phi(k)$$

$$+ \frac{e}{\sqrt{N}} \sum_j \int \frac{d^{d+1}k\, d^{d+1}q}{(2\pi)^{2d+2}}\, \phi(q)\, \bar{\Psi}_j(k+q)\, \gamma_0 \Psi_j(k)$$

Interaction vertex contains
γ_0 instead of i $\gamma_{d\text{-}m}$

Values of $\mathbf{d_c}$ & critical exponents same as Ising-nematic case

[**IM**, *Phys. Rev. Research 2, 043277 (2020)*]

2 Fermion Flavours + $U_c(1) \times U_s(1)$

Model for QCPs for Mott insulator to metal & metal to metal transitions

[L. Zou & D. Chowdhury, *Phys. Rev. Research 2, 023344 (2020)*]

- First fermion couples to the gauge fields a_c & a_s as ($e^c a_c + e^s a_s$)

- Second fermion couples as ($e^c a_c - e^s a_s$)

- At one-loop, beta functions for the effective coupling constants give a **fixed line** ($e^c_{\text{eff}} + e^s_{\text{eff}}$) $\propto \epsilon$

- m > 1 ☛ fixed line feature survives at generic loops
  [**IM**, Phys. *Rev. Research 2, 043277 (2020)*]

- m = 1 ☛ fixed line feature breaks at three-loop
  [**IM**, *Phys. Rev. Research 2, 043277 (2020)*]

NFLs: Other Examples from My Work

Luttinger semimetals have quadratic band crossings

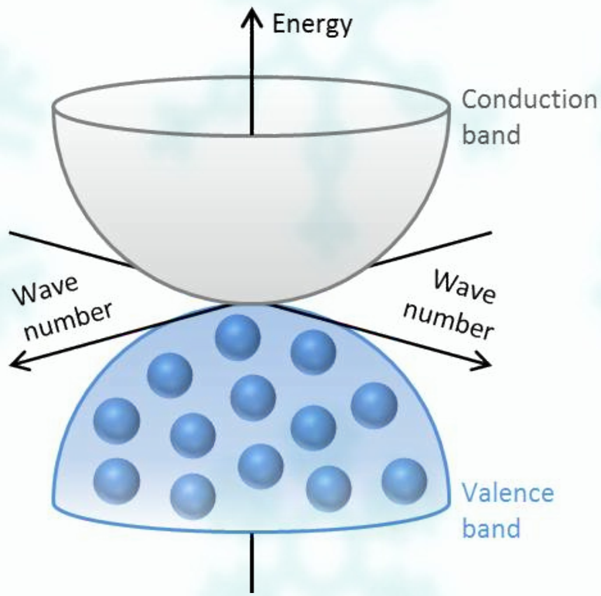

[Nakatsuji]

Gray Tin

HgTe

$Pr_2Ir_2O_7$

- Coulomb interactions drive it to NFL
  ☛ Luttinger-Abrikosov-Beneslavskii phase

- NFL unstable to disorder
  [R. M. Nandkishore & S. A. Parameswaran, *PRB (2017)*;
  IM & R. M. Nandkishore, *PRB (2018)*]

- Optical, dc, thermal conductivities
  + thermoelectric coefficient computed
  [**IM** & H. Freire, *PRB (2021)*; H. Freire & **IM**, *Phys. Lett. A (2021)*]

NFLs: Other Examples from My Work

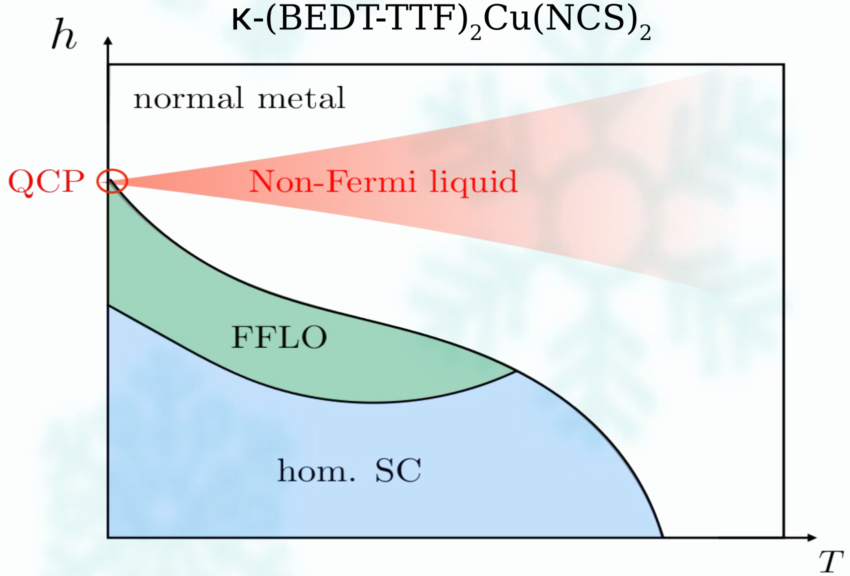

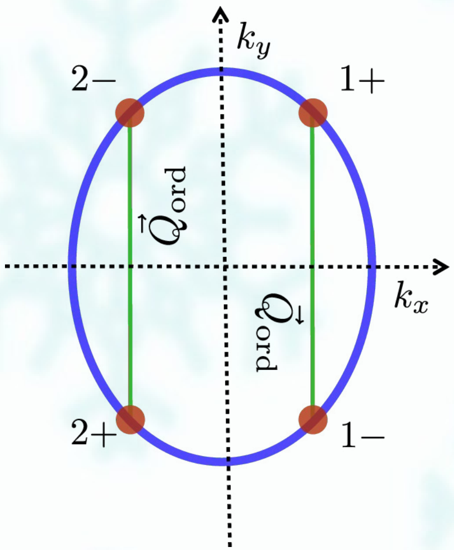

Fermi Surface
+
FFLO Boson

[D. Pimenov, **IM**, F. Piazza, M. Punk, *PRB (2018)*]

Fermi Surface
+
Spin Density Wave

[**IM**, *Ann. Phys. (2015)*]

Collective Excitations of Critical Fermi Surface

Zero Sound for FL

Collective Mode in Collisionless Regime for Neutral FL

- Collective mode ☛ density oscillation with wavevector **q** & frequency **ν**
- **ν** >> Frequency of quasiparticle collisions **ω**
- Damping of zero sound from quasiparticle collisions negligible
- Excitations are localized close to the Fermi level
- Corresponds to an anisotropic redistribution of quasiparticles around the Fermi surface
- Transitions to first sound in the hydrodynamic regime (**ν** << **ω**)

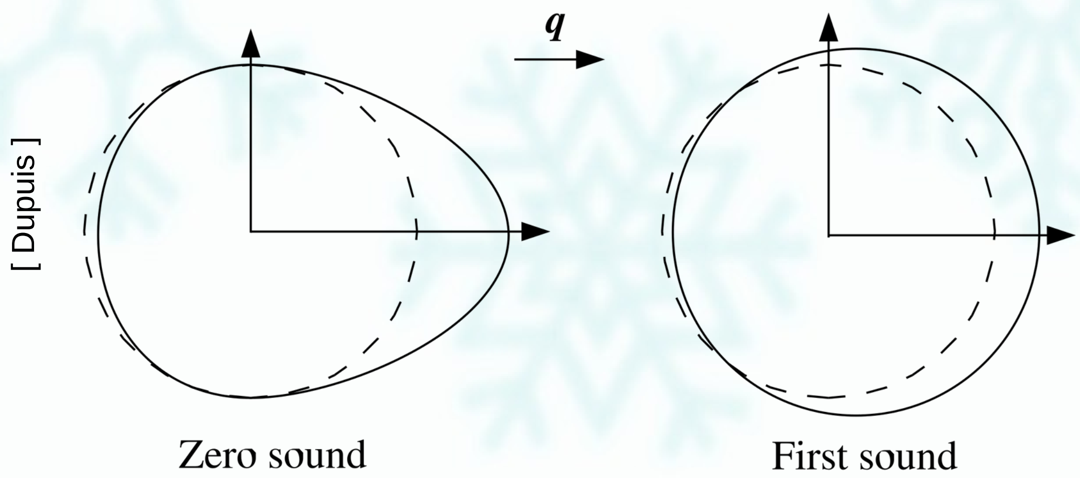

Quantum Boltzmann Eqns (QBE)

Collective Mode in Collisionless Regime for Neutral FL

- FL ☛ QBE of quasiparticles provides information about the low-energy excitations ☛ E.O.M. of nonequilibrium Green's function

- Conventional derivation of the QBE relies on existence of quasiparticles:

spectral function

$$\xi_{\mathbf{k}} = \frac{k^2}{2\,m} - k_F\,, \qquad A(\omega, \xi_{\mathbf{k}}, \theta_{\mathbf{k}}) = \frac{-2\,\mathrm{Im}\Sigma^R(\omega,\xi_{\mathbf{k}})}{[\omega-\xi_{\mathbf{k}}-\mathrm{Re}\Sigma^R(\omega,\xi_{\mathbf{k}})]^2+[\mathrm{Im}\Sigma^R(\omega,\xi_{\mathbf{k}})]^2}$$

$$\mathrm{Im}\ \Sigma^R \sim \omega^2 \ll |\omega| \text{ for } |\omega| \ll 1 \Rightarrow A \simeq 2\,\pi\,\delta\big(\omega - \xi_{\mathbf{k}} - \mathrm{Re}\Sigma^R\big)$$

$$\mathrm{G}_0^< = i\,f_0(\omega)\,A\,, \qquad \delta f \equiv f(\omega, \theta_{\mathbf{k}}; t, \mathbf{r}) - f_0\,, \qquad \delta u(\theta_{\mathbf{k}}; t, \mathbf{r}) \sim \int d\xi_{\mathbf{k}}\,\delta f$$

linearized QBE

Fermi surface deformation

- E.O.M. of δf or δu ☛ fails for NFLs

QBE for NFLs

$$\text{Im } \Sigma^R \sim |\omega|^{2/3} \gg |\omega| \text{ for } |\omega| \ll 1$$

- Spectral function A no longer a delta function
- f does not satisfy a closed E.O.M even at equilibrium
- Way out ☛ if self-energy is function of ω only, A is a sharply peaked function of ξ_k

Generalized distribution function

$$\text{-i}\int \frac{d\xi_{\mathbf{k}}}{2\pi}\, G^<(\omega, \xi_{\mathbf{k}}, \theta_{\mathbf{k}}; t, \mathbf{r}) \equiv f(\omega, \theta_{\mathbf{k}}; t, \mathbf{r})$$

[Prange & Kadanoff, 1964]

- E.O.M. of generalized Fermi surface deformation

$$\delta u(\theta_{\mathbf{k}}; t, \mathbf{r}) = \int \frac{d\omega}{2\pi}\, \delta f(\omega, \theta_{\mathbf{k}}; t, \mathbf{r})$$

$$\delta u_\ell = \int \frac{d\theta}{2\pi}\, \delta u(\theta; t, \mathbf{r})\, e^{i\ell\theta}$$

QBE for Ising-Nematic QCP

$$F_{Landau}(\omega_k, \theta) = e^2\, m\, \mathrm{Re}\Big[D^R_{1-loop}(\omega_k, |\theta|)\Big] = \frac{e^2\, m\, k_F^4\, \theta^4}{k_F^6\, \theta^6 + \frac{e^4\, m^2\, {\omega_k}^2}{\pi^2\, v_F^2}}$$

$$\nu\, \delta u_\ell(\nu, \mathbf{q}) = v_F\, |\mathbf{q}|\, \frac{\delta u_{\ell+1}(\nu, \mathbf{q}) + \delta u_{\ell-1}(\nu, \mathbf{q})}{2\left(1 + \frac{F_0 - F_\ell}{\pi}\right)}$$

Zero sound ☛ $\ell = 0$ channel

$$\nu = \frac{\pm\sqrt{2\,\pi}\, v_F\, |\mathbf{q}|}{\sqrt{\pi + 4\, F_{01} - 2\, F_{02} + \sqrt{4\, F_{02}^2 + 12\,\pi\, F_{02} - 8\,\pi\, F_{01} + \pi^2}}}$$

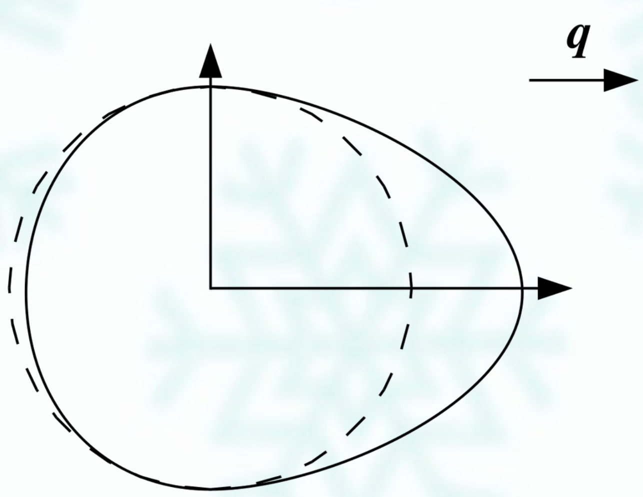

Zero sound

[**IM**, *arXiv (2021)*]

Charged NFL: Plasmons

$$\left(\nu + i\,\gamma\,\delta_{|\ell|>1}\right)\delta u_\ell(\nu,\mathbf{q}) = -\sigma_3\,v_F\,|\mathbf{q}|\,\frac{\delta u_{\ell+1}(\nu,\mathbf{q}) + \delta u_{\ell-1}(\nu,\mathbf{q}) + F_c\,u_0\,\delta_{|\ell|,1}}{2\left(1+\frac{F_0-F_\ell}{\pi}\right)}$$

$$F_c = \frac{2\,\pi\,\alpha}{\lambda_F\,|\mathbf{q}|}$$

Coulomb via RPA

- Plasmon ☛ $\ell = 0$ channel, $\mathbf{q} \to 0$

$$\nu = \frac{\pm\,\pi\,v_F\,\sqrt{|\mathbf{q}|}\,\sqrt{\frac{2\,\alpha}{\lambda_F}}}{\sqrt{\pi+2\,F_{01}-F_{02}+\sqrt{(F_{02}+\pi)^2}}} - i\,\gamma\,\frac{\lambda_F\,|\mathbf{q}|}{8\,\pi\,\alpha}$$

- Transitions to zero sound of neutral NFL for larger **q**

[**IM**, *arXiv (2021)*]

Moiré Superlattices

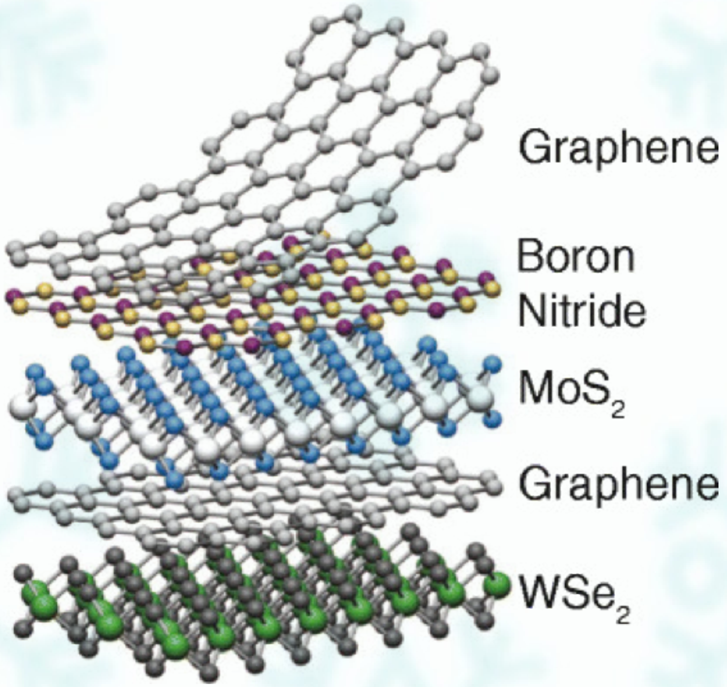

[Geim]

Moiré Superlattices

2 or more atomically-thin sheets of periodic patterns overlaid with a relative twist or a mismatched lattice constant
☛ (Quasi)-periodic interference pattern

Twisted Bilayer Graphene

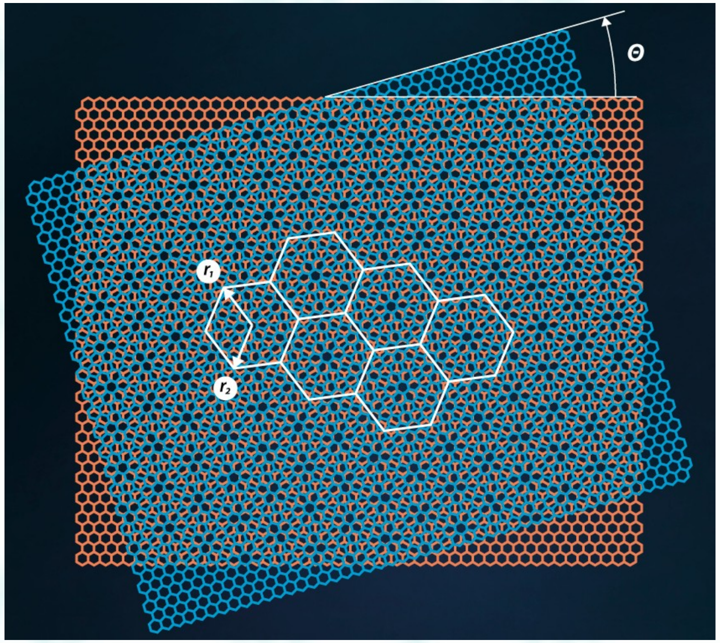

[MIPT]

Aligned Graphene-hBN

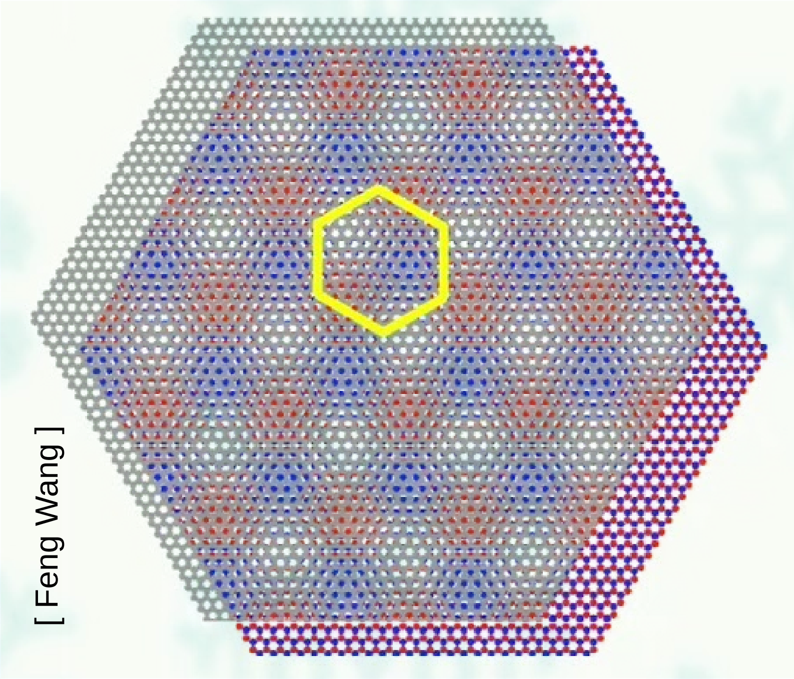

[Feng Wang]

- **Experimentally realized by stacking 2D materials**
- **Enlarged unit cell**

Magic-Angle Twisted Bilayer Graphene

- For small twist-angles $\theta \sim 1^{\circ}$
  ☛ large moiré unit cell ~ 10^4 atoms (10 nm)
- 3 notable regions: AA, AB, BA, each forming a triangular lattice
- AB and BA sites together form a honeycomb lattice
- Show insulating behavior when moiré bands are partially filled

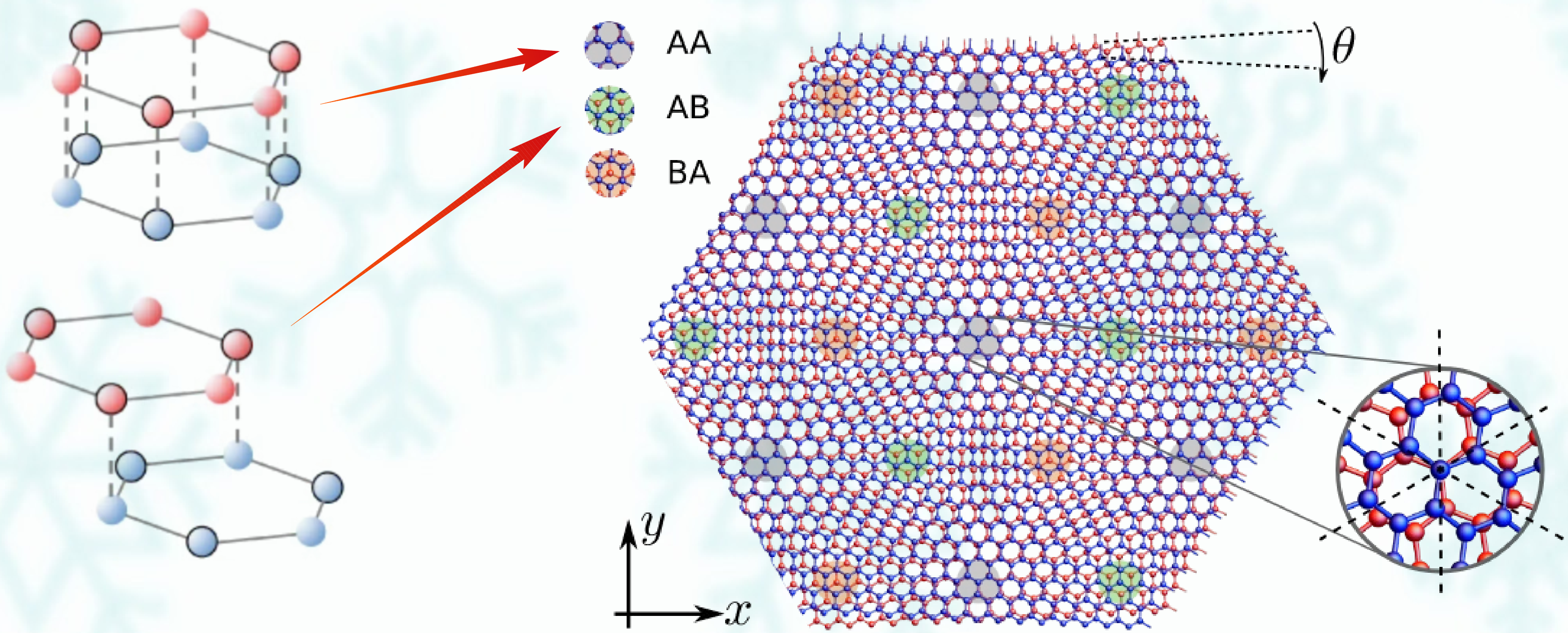

[Thomson et al (2018)]

Platform for Strong Correlations

- Moire periodicity >> larger than either lattice constant
- Increase in lattice length ☛ electron propagates at a longer wave length on the lattice ☛ lower momentum / reduced K.E.
- Interaction energy >> K.E.
- Magic angles ☛ bands near charge neutrality become nearly flat

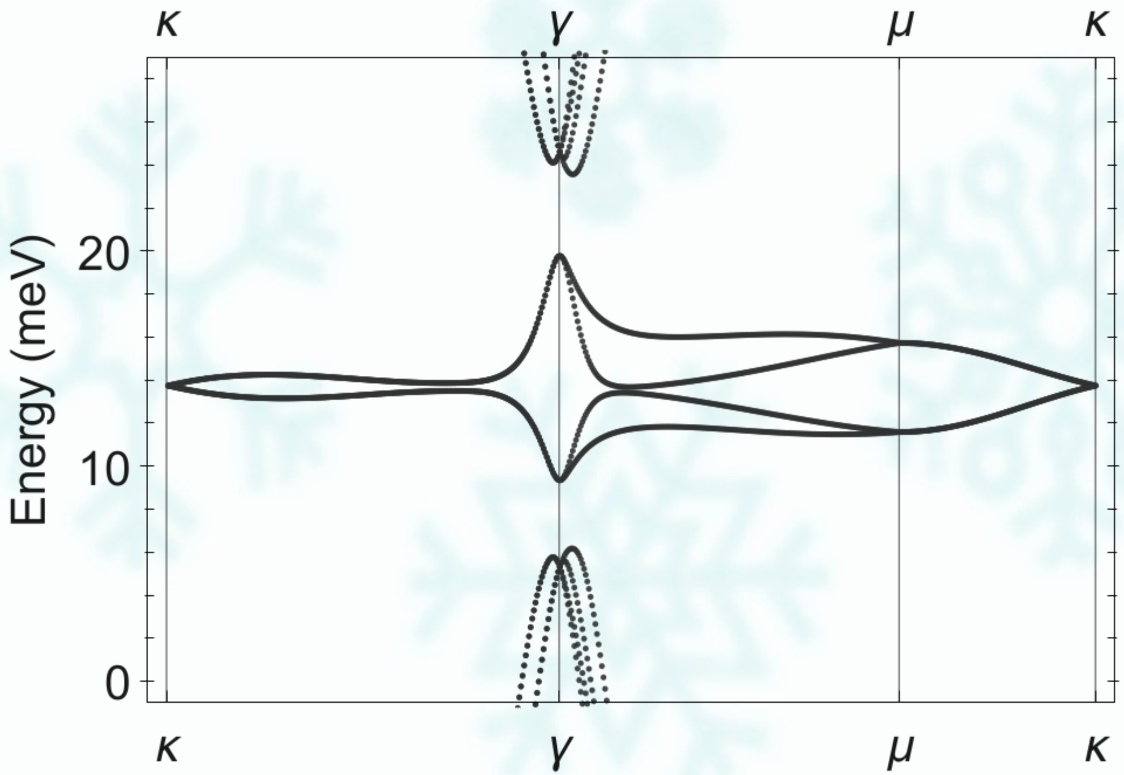

[Black-Scahffer et al (2021)]

Low energy band structure of TBG at θ ≈ 1.2°

Moiré: Simpler + Highly Tunable

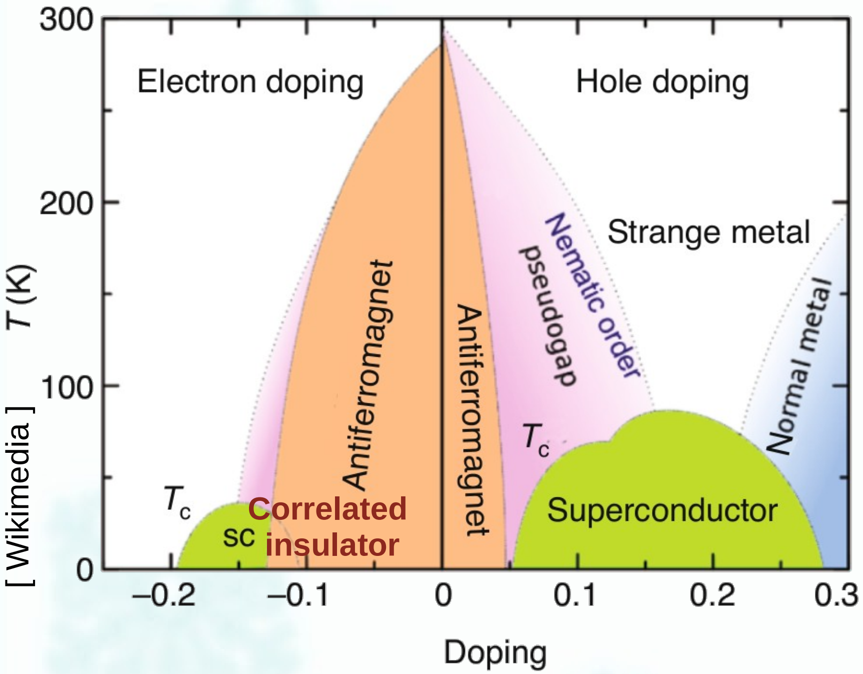

Phase diagram of cuprates

New insights into high-T_c & strange metals?

Magic-Angle Twisted Bilayer Graphene

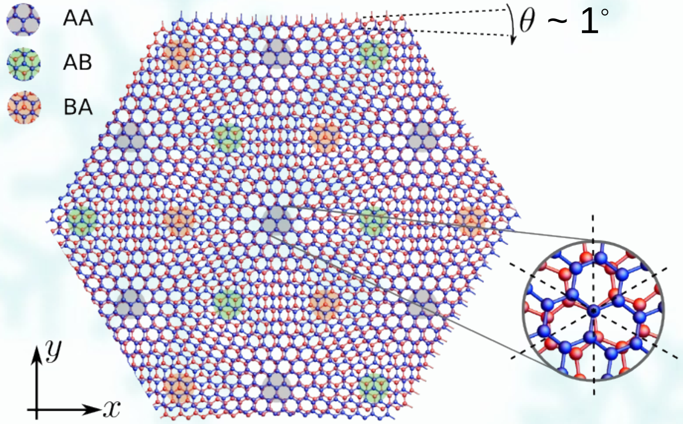

[Thomson et al (2018)]

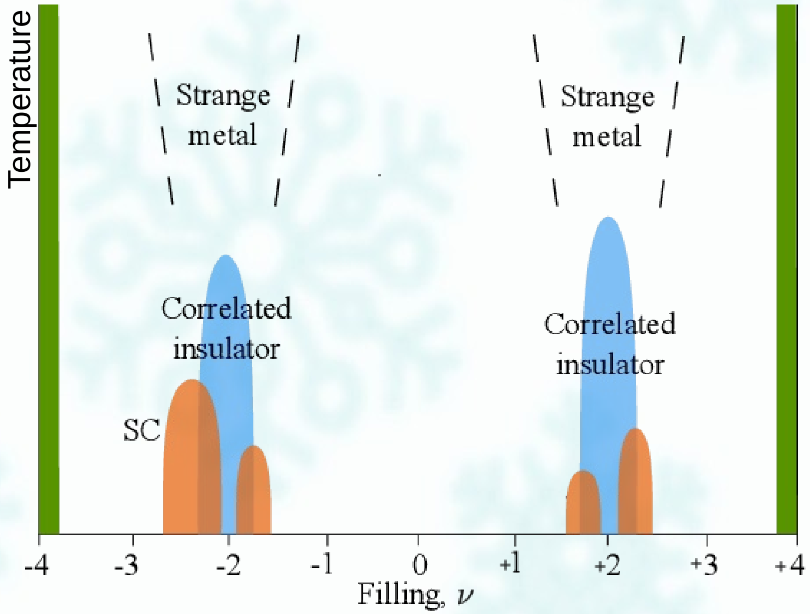

Correlated insulators at half-fillings

[Cao et al (2019)]

Chemical complexity replaced by structural complexity

Moiré: My Recent Work

Magic-Angle Twisted Bilayer Graphene

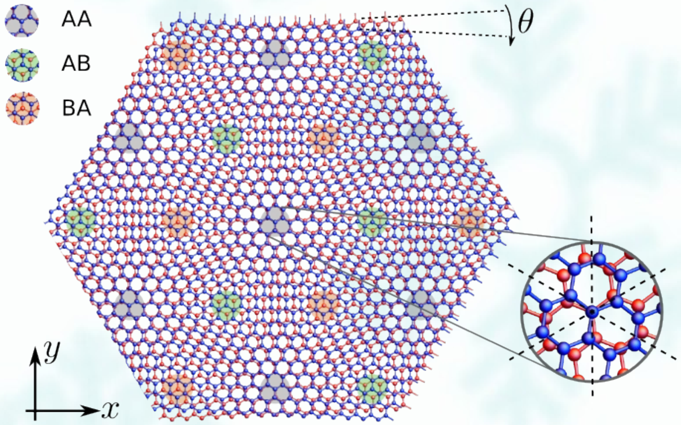

Thomson et al (2018)

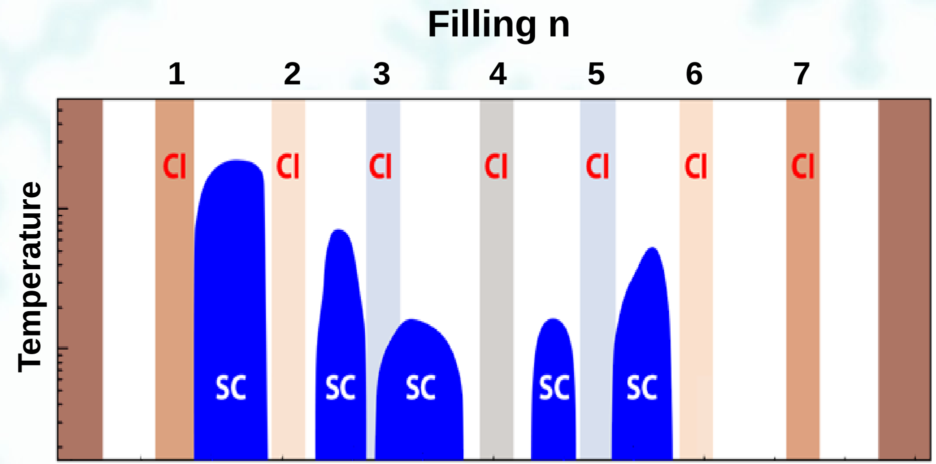

MacDonald (2019)

Correlated insulators (**CI**)

at integer fillings

[**IM**, J. Yao, E. J. Mueller, *PRB (2021)*]

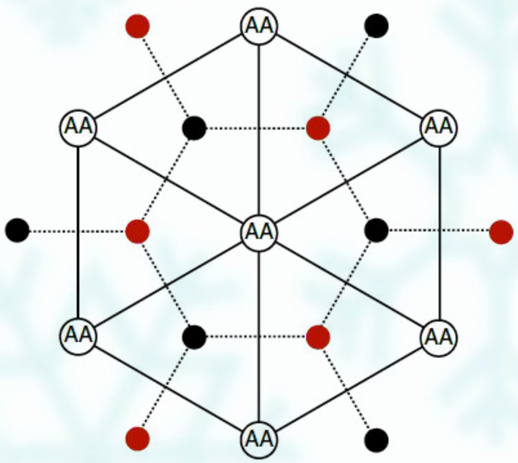

8 states per moiré unit cell:

2 (spin) x 2 (sublattice) x 2 (valley)

Identify static charge configurations

A Simple Model

- **Full lattice model is challenging ~ 10^4 bands**
- **Electronic structure of low-energy bands built from Wannier orbitals centered at AB & BA sites**
- **Each Wannier state has a 3-lobed spatial structure ☛ each lobe centered on an AA site** [Koshino et al, Phys. Rev. X 8, 031087 (2018)]
- **In addition to sublattice index (AB or BA), Wannier states labelled by spin and valley indices ☛ 8-band effective Hamiltonian**

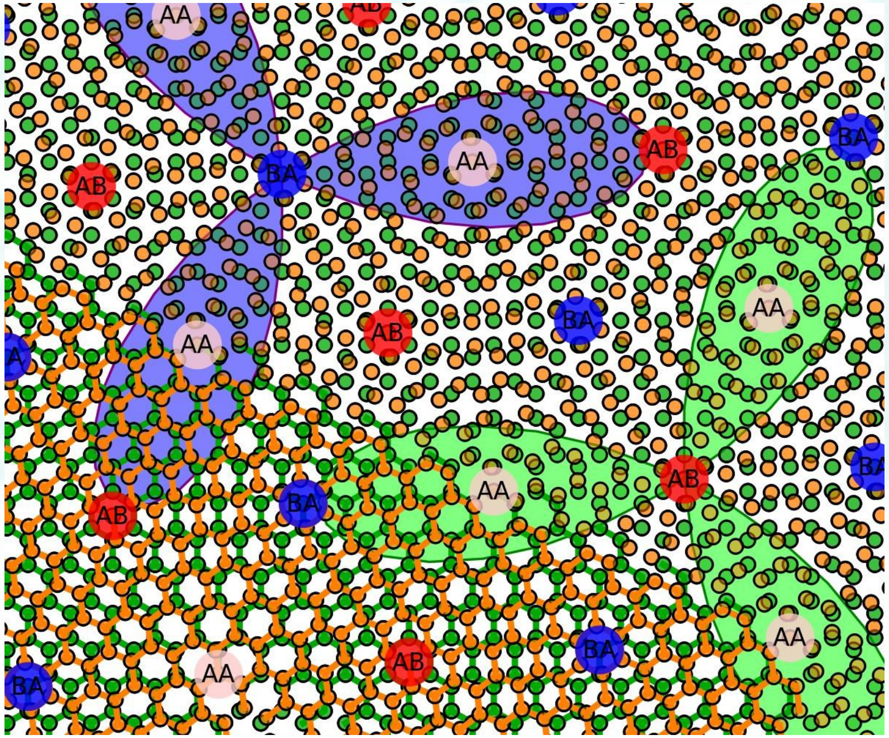

Subtleties

- **There is a topological obstruction that prevents the existence of exponentially localized Wannier states obeying all the emergent symmetries**

- **Wannier states that we work with are exponentially localized, with one of the protecting symmetries broken**

- **These considerations only affect physics on an exponentially small energy scale: irrelevant to the questions we are asking**

[Wang and Vafek, *PRB (2020)*]

Energy Scales

- **Effective electronic hopping matrix element between two nearest Wannier orbitals ~ 0.3 meV**

- **Effective direct Coulomb interaction between them ~10 meV**

[Koshino et al, *PRX (2018)*]

- **We neglect kinetic energy and find stationary charge configurations which minimize the Coulomb interaction energy**

Procedure

- Consider periodic arrangements of charges defined by the generators $\mathbf{v}_1 = \mathbf{m}_1\, \mathbf{a}_1 + \mathbf{m}_2\, \mathbf{a}_2$ and $\mathbf{v}_2 = \mathbf{n}_1\, \mathbf{a}_1 + \mathbf{n}_2\, \mathbf{a}_2$
- We include all unit cells containing fewer than 13 sublattice sites, with $\mathbf{m}_1, \mathbf{m}_2, \mathbf{n}_1, \mathbf{n}_2 <= 4$
- In all, we consider well over 3000 charge configurations

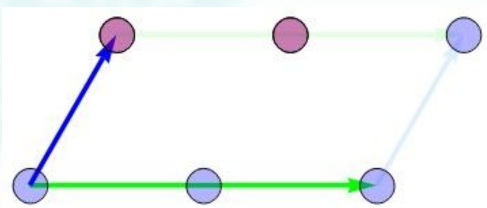

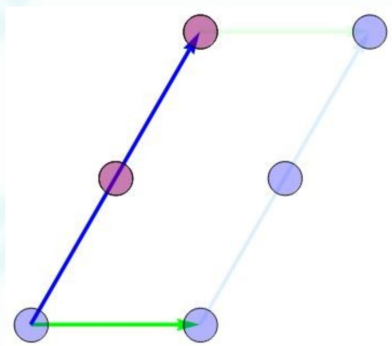

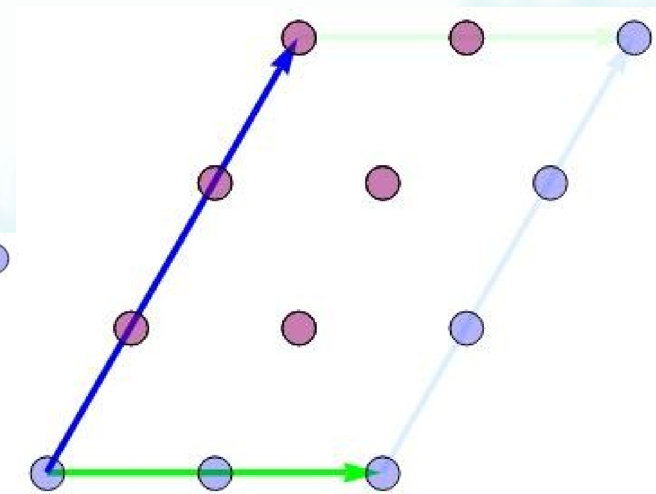

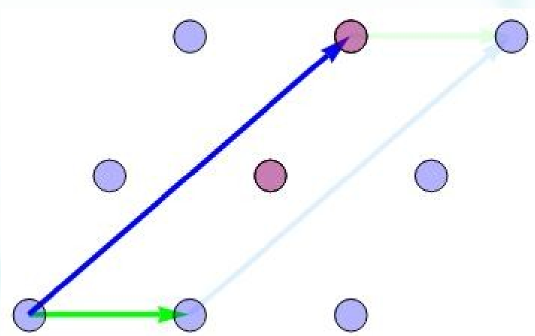

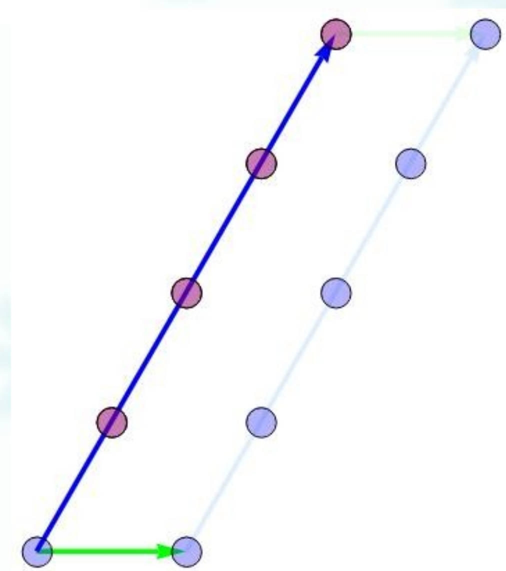

Procedure ...

- **For a single electron, each of the 3 lobes of a Wannier orbital accommodates a charge of -e/3 (fracton)**

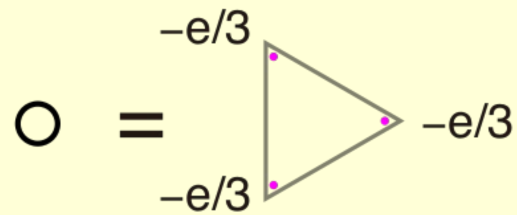

- **Coulomb interaction energy from the fractons well approximated by**

$$V_{ij} = \begin{cases} \frac{e^2}{9\,\epsilon\,L_M}\,\frac{1}{|r_i - r_j|} & r_i \neq r_j \\ \frac{e^2}{9\times 0.28\,L_M} & r_i = r_j \end{cases}$$

for two fractons located at the same lobe

- **We include exchange interaction that lowers energy by *J* when two overlapping occupied orbitals have same spin and valley quantum numbers (Hund's rule)**

[Koshino et al, *PRX (2018)*]

Procedure ...

- Coulomb interaction energy from a 2D array of charges is linearly divergent with system size
- The relative energies of the configurations with the same average density, however, are well defined
- After subtracting off the leading divergence, the remaining sums regularized by using 2D Ewald sums

Moiré: My Recent Work

Magic-Angle Twisted Bilayer Graphene

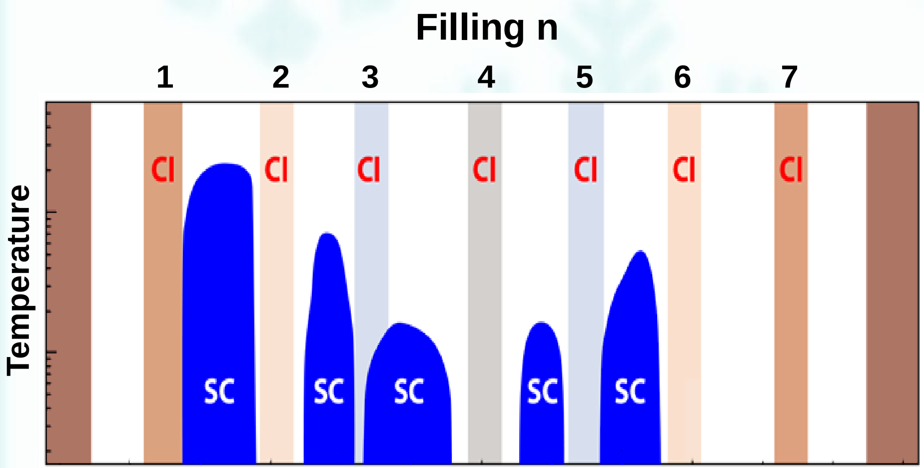

MacDonald (2019)

Correlated insulators (**CI**)

at integer fillings

of 8 moiré bands

Identify static charge configurations

E.g. n = 1

Which one has lowest energy?

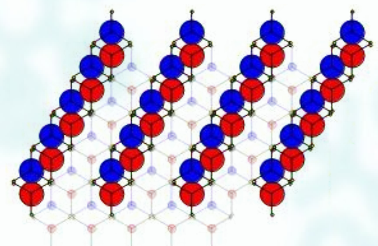

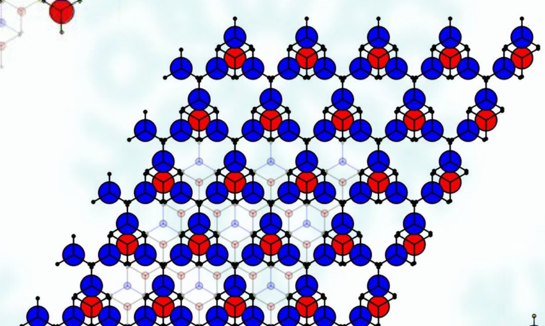

> 3000 possible states

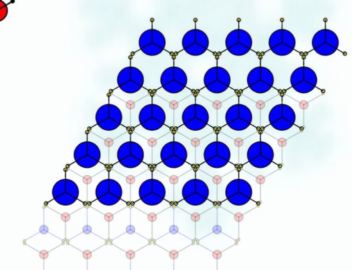

e- at AB site

e- at BA site

[**IM**, J. Yao, E. J. Mueller, *PRB (2021)*]

Ground States

Energy minimization

Striped Ferromagnet
☛ Ground State at n = 1

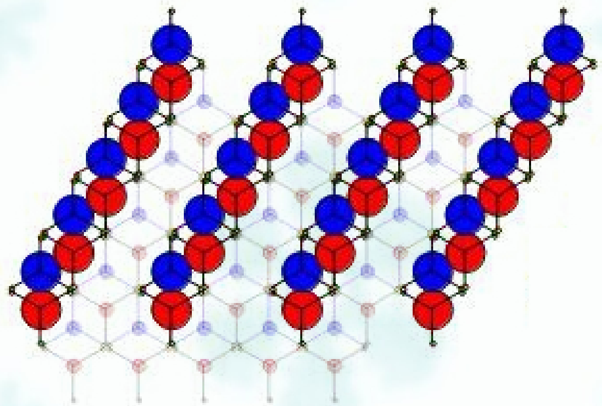

[**IM**, J. Yao, E. J. Mueller, *PRB (2021)*]

Agrees with experiments

[Zondiner et al, *Nature (2020)*]
[Choi et al, *Nature (2019)*]
[Lu et al, *Nature (2019)*]

Excitations

Energy of 4 types of excitations:

- adding a single electron
- removing a single electron
- creating an electron-hole pair
- flipping spin / valley of a single electron

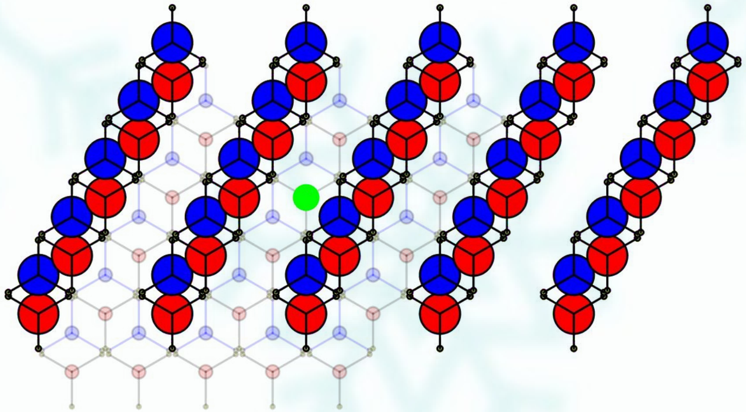

Current + Future Plan

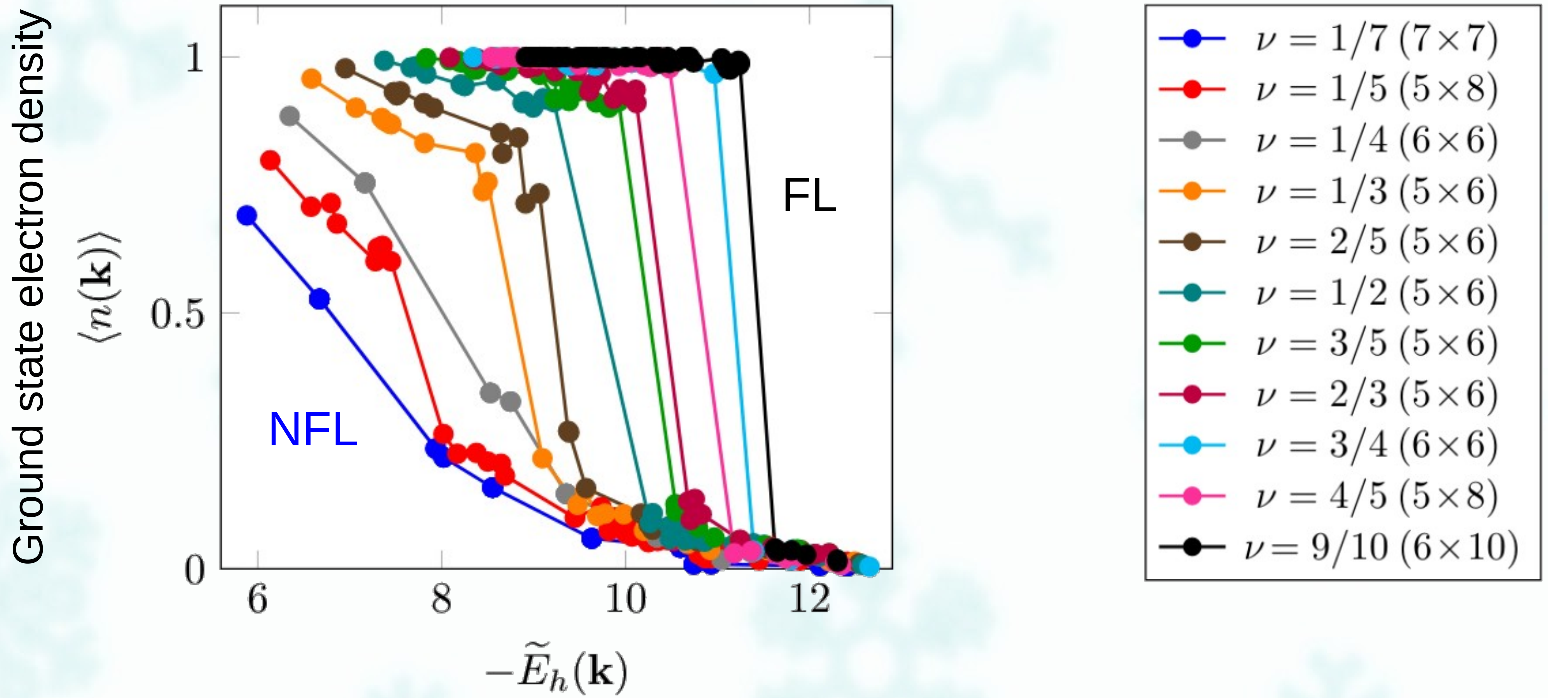

[A. Abouelkomsan, Z. Liu, & E. J. Bergholtz, *PRL (2020)*]

Interaction-driven FL / NFL in ABC-stacked trilayer graphene
at fractional fillings ν

- **Identify possible ordering instabilities**
- **Compute free energy to find the ground states**
- **Construct a field theory action to derive RG equations**

International Collaborations

Yukawa-SYK Models

Yuxuan Wang
University of Florida

Superconductivity mediated by antiferromagnetic magnons

Akashdeep Kamra
IFIMAC, Universidad Autónoma de Madrid

Transport in 2d / 3d structures

Klaus Zeigler
Universität Augsburg

Order parameters in moiré lattices

Rafael M. Fernandes
Uni. of Minnesota

Fractionally-filled moiré flat-bands

Emil J. Bergholtz
Stockholm Uni.

Twisted Bilayer Cuprates

Annica Black-Schaffer
Uppsala Uni.

and others. . .

Thank you for your attention!

54 Papers

16 single auth.

16 major collabs.

Quantum Condensed Matter

with a focus on

Strongly Correlated Systems

Strange Metals

or

Non-Fermi liquids

2d multi-layers

☛ **Moiré superlattices**

Procedure ...

- Coulomb interaction energy from a 2D array of charges is linearly divergent with system size
- The relative energies of the configurations with the same average density, however, are well defined
- After subtracting off the leading divergence, the remaining sums regularized by using 2D Ewald sums

$$\sum_{\mathbf{w}\in\mathcal{L}} \frac{1}{|\mathbf{r}-\mathbf{w}|} = f_s(\mathbf{r}) + f_l(\mathbf{r}) + C$$

$$f_s = \sum_{\mathbf{w}\in\mathcal{L}} \frac{1}{|\mathbf{r}-\mathbf{w}|}\,\mathrm{erfc}\left(\frac{|\mathbf{r}-\mathbf{w}|}{2\eta}\right) - \frac{4\sqrt{\pi}}{\Omega}\eta$$

$$f_l = \frac{2\pi}{\Omega} \sum_{\mathbf{k}\in\bar{\mathcal{L}}\setminus 0} \frac{e^{\mathrm{i}\,\mathbf{k}\cdot\mathbf{r}}}{2\,k}\,\mathrm{erfc}\,(k\,\eta)$$

Sum is over a Bravais lattice generated by the supercell vectors $\mathbf{v}_1$, $\mathbf{v}_2$